

Modeling the Rate of Heterogeneous Reactions

To appear in:

“Modeling of Heterogeneous Catalytic Reactions: From the molecular process to the technical system”

O. Deutschmann (Ed.), Wiley-VCH, Weinheim 2011

Lothar Kunz, Lubow Maier, Steffen Tischer, Olaf Deutschmann*

Karlsruhe Institute of Technology (KIT)

Version 28.03.2011

*To whom correspondence should be addressed:

Prof. Dr. Olaf Deutschmann
Chair Chemical Technology at Karlsruhe Institute of Technology (KIT)
Engesserstr. 20, 76131 Karlsruhe, Germany

Tel.: +49 721 608-43138, Fax: -44805, Sekr. Tel.: -43064, -42121
Email: deutschmann@kit.edu

Modeling the Rate of Heterogeneous Reactions

Lothar Kunz, Lubow Maier, Steffen Tischer, Olaf Deutschmann

1 Introduction

This chapter discusses links and still-existing gaps between modeling surface reaction rates on a fundamental, molecular-based approach on the one side and on a practical reaction engineering approach on the other.

The mechanisms of heterogeneously catalyzed gas-phase reactions can in principle be described by the sequence of elementary reaction steps of the cycle, including adsorption, surface diffusion, chemical transformations of adsorbed species, and desorption, and it is the basis for deriving the kinetics of the reaction. In the *macroscopic* regime, the rate of a catalytic reaction is modeled by fitting empirical equations, such as power laws, to experimental data to describe its dependence on concentration and pressure and to determine rate constants that depend exponentially on temperature. This approach was used in chemical engineering for reactor and process design for many years^[1].

Assumptions on reaction schemes (kinetic models) provide correlations between surface coverages of intermediates and the external variables. Improved kinetic models could be developed when atomic processes on surfaces and the identification and characterization of surface species became available. Here, the progress of a catalytic reaction is described by a *microkinetics* approach by modeling the macroscopic kinetics by means of correlations of the atomic processes with macroscopic parameters within the framework of a suitable continuum model^[2, 3]. Continuum variables for the partial surface coverages are, to a first approximation, correlated to external parameters (partial pressures and temperature) by the mean-field

approximation of a surface consisting of identical non-interacting adsorption sites. Because of this idealization of the catalytic process, the continuum model can describe the reaction kinetics only to a first approximation neglecting interactions between adsorbed species and non-identical adsorption sites. Apart from the heterogeneity of adsorption sites, the surfaces may exhibit structural transformations.

The Langmuir – Hinshelwood – Hougen –Watson (LHHW) model has been a popular simplified approach of the mean-field approximation for modeling technical catalytic reactors for many years. It is based on a continuum model, in which the surface of the catalyst is described as an array of equivalent sites which do interact neither before nor after chemisorption. Furthermore, the derivation of rate equations assumes that both reactants and products are equilibrated with surface species and that a rate-determining step can be identified. Surface coverages are correlated with partial pressures in the fluid phase by means of Langmuir adsorption isotherms. Despite these over-simplifications, the LHHW kinetics model has been used for reactor and process design in industry until today. The kinetic parameters which are determined by fitting the rate equations to experimental data, however, do not have physical meanings in general. Sometimes even less complicated simple power-law kinetics for straightforward reactions (e.g., $A + B$) are used.

On the most fundamental level, Density Functional Theory (DFT), Molecular Dynamics (MD), and Monte Carlo (MC) simulations are used to elucidate the molecular aspects of heterogeneous catalysis as discussed in the previous three Chapters. Table 1 lists methods for modeling the chemical reaction rate of heterogeneous catalytic reactions in a hierarchical order.

A major objective of current research in catalysis is the development of methods that allow the incorporation of the molecular understanding of catalysis into the modeling of technical reactors. In principle, ab-initio and DFT calculations can provide information that are fed into Monte Carlo (MC) simulations of catalytic processes on individual nanoparticles, which then can compute surface reaction rates as function of the local (fluid-phase) partial pressures, temperature and adsorbate structure. These rates have then still to be applied in models tractable for the simulation of technical systems. Hence, the gap still to be bridged in modeling technical systems is between MC simulations and reactor simulation. In the last two decades, the mean-field approximation (MF) has been used as work-around in order to overcome the much simpler Langmuir-Hinshelwood or even power-law approaches and to include some of the elementary aspects of catalysis into models suitable for numerical simulation of catalytic reactors.

This Chapter focuses on two major items: MC simulations as potential tool for the derivation of surface reaction rates and the MF approach as state-of-the-art modeling of reaction rates in technical systems. Eventually, a local chemical source term, R_i^{het} , is needed that provides the specific net rate of the production of species i due to heterogeneous chemical reactions at a certain macroscopic position of a catalytic surface in the technical reactor. This source term as function of the local conditions can then be implemented into fluid dynamics and heat transport simulations of the technical system, which will be discussed in the next Chapters.

Since elementary-step reaction mechanisms were first introduced in modeling homogeneous reaction systems and since homogeneous reactions in the fluid phase do also play a significant role in many technical catalytic reactors, this chapter will start with a short introduction on the well-established approach of modeling the rates of chemical reactions in the gas phase.

2 Modeling the rates of chemical reactions in the gas phase

In many catalytic reactors, the reactions do not exclusively occur on the catalyst surface but also in the fluid flow. In some reactors, even the desired products are mainly produced in the gas phase, for instance in the oxidative dehydrogenation of paraffins to olefins over noble metals at short contact times and high temperatures^[4-11]. Such cases are dominated by the interaction between gas-phase and surface kinetics and transport. Therefore, reactor simulations often need to include an appropriate model for the homogeneous kinetics along with the heterogeneous reaction models. The species governing equations in fluid flow simulations usually contain a source term such as R_i^{hom} denoting the specific net rate of production of species i due to homogeneous chemical reactions. Considering a set of K_g chemical reactions among N_g species A_i

$$\sum_{i=1}^{N_g} \nu'_{ik} A_i \rightarrow \sum_{i=1}^{N_g} \nu''_{ik} A_i, \quad (2.1)$$

with ν'_{ik}, ν''_{ik} being the stoichiometric coefficients, and an Arrhenius-like rate expression, $AT^\beta \exp(-E_a R^{-1} T^{-1})$, this source term can be expressed by

$$R_i^{\text{hom}} = M_i \sum_{k=1}^{K_g} (\nu''_{ik} - \nu'_{ik}) A_k T^{\beta_k} \exp\left[\frac{-E_{a_k}}{RT}\right] \prod_{j=1}^{N_g} \left(\frac{Y_j \rho}{M_j}\right)^{a_{jk}}. \quad (2.2)$$

Here, A_k is the pre-exponential factor, β_k is the temperature exponent, E_{a_k} is the activation energy, and a_{jk} is the order of reaction k related to the concentration of species j . The advantage of the application of elementary reactions is that the reaction orders a_{jk} in Eq. (2.2) equal the stoichiometric coefficients ν'_{jk} .

Various sets of elementary reactions are available for modeling homogeneous gas phase reactions, for instance for total^[12] and partial oxidation, and pyrolysis^[13, 14] of hydrocarbons.

Table 2 lists a selection (far from being complete) of gas-phase reaction mechanisms, which may also be considered in the simulation of heterogeneous chemical systems.

Even though the implementation of Eq. (2.2) into CFD codes for the simulation of chemical reactors is straightforward, an additional highly nonlinear coupling is introduced into the governing equations leading to considerable computational efforts. The nonlinearity, the large number of chemical species, and the fact that chemical reactions exhibit a large range of time scales render the solution of those equation systems challenging. In particular for turbulent flows, but sometimes even for laminar flows, the solution of the system is too CPU time-consuming with current numerical algorithms and computer capacities. This calls for the application of reduction algorithms for large reaction mechanisms, for instance through the extraction of the intrinsic low dimensional manifolds of trajectories in chemical space ^[15]. Another approach is to use “as little chemistry as necessary”. In these so-called adaptive chemistry methods, the construction of the reaction mechanism only includes steps relevant for the application studied ^[16].

3 Computation of surface reaction rates on a molecular basis

In this section, we discuss the derivation of rates of heterogeneous reactions from a molecular point of view. Since the previous chapters have already discussed in detail DFT, MD, and kMC simulations, we focus on ways to make such molecular methods - in particular MC simulations - a useful tool for simulation of technical systems.

3.1 Kinetic Monte Carlo Simulations

From a macroscopic point of view, effects on overall reaction rates resulting from lateral interactions of the adsorbates are inherently difficult to treat. In the mean-field approximation,

as discussed below, they are either neglected or incorporated by mean rate coefficients. If the specific adsorbate-adsorbate interactions are understood quantitatively, then (kinetic) Monte Carlo ((k)MC) simulations can be carried out.

From a microscopic point of view, the coarse graining of rates for chemical reactions starting from elementary processes requires averaging over many reaction events. As rare events chemical reactions require a long simulation time, which limits the use of Molecular Dynamics (MD) simulations and requires methods like kinetic Monte Carlo simulations.

MC simulations today appear as the model of choice to bridge the gap between molecular modeling and reactor modeling. Therefore, this section is specifically devoted to MC simulations that try to more and more include effects of real catalytic particles such as the three-dimensional structure of the catalyst nanoparticles, support and spill-over effects. Since MC simulation is the specific topic of the previous chapter, only the principles need to be summarized at the beginning of this section.

In MC simulations for surface processes (Fig. 1), the evolution of the surface coverage configuration is calculated as a correct sequence in time. The foundation of this method is the master equation:

$$\frac{dP_\alpha}{dt} = \sum_\beta [k_{\alpha\beta} P_\beta - k_{\beta\alpha} P_\alpha]. \quad (3.1)$$

This equation describes the evolution of the probability P_α for the system being in the surface configuration state α . Here, $k_{\alpha\beta}$ defines the transition probability from state α to state β . The transition in the sense of surface simulation can for instance be a diffusion step or a reaction with rate $k_{\alpha\beta}$. Analytical solutions to the master equation can only be derived for simple cases. In general, a numerical solution is required. A MC simulation starts from a state

α and repeatedly picks a random possible process and advances in time. Averaging over several trajectories leads to a numerical solution of the master equation.

The time step and process have to be chosen in accordance with the likelihood that state α is left and that a specific process has occurred. Two main algorithms have been developed, the variable step size method (VSSM) and the first reaction method (FRM). In the VSSM the time increment Δt is derived from a uniform random number r on $(0,1]$ by

$$\Delta t = -\frac{\ln r}{\sum_{\beta} k_{\beta\alpha}} . \quad (3.2)$$

The process is picked independently from the time step at a likelihood k/k_{total} , where k is the rate of the picked process and k_{total} is the sum of all processes which can start from the current state. In the FRM for every possible process with rate k starting from state α , a time increment

$$\Delta t = -\frac{\ln r}{k} \quad (3.3)$$

is drawn and finally the process with the smallest Δt is chosen as next step. A variant of the VSSM method is called random site method (RSM). For this a site, a process, and a time increment are picked independently. With a probability of $k/\max_p k_p$, the process is performed. VSSM is the most widely used method, also known as n-fold way or BKL method after Bortz, Kalos, and Libowitz ^[17]. In general, the choice of algorithm depends on the specific problem. In some cases a combination of the variants leads to a good performance ^[18].

3.2 Extension of MC simulations to nanoparticles

The description of the surface configuration requires only a mapping from adsorption sites to species. The layout of the sites can be a lattice, like crystal surfaces, but also off-lattice. The widely used lattices originate from the periodic surfaces resulting in a low number of processes since they are independent of their global location.

But catalytic surfaces are certainly non-uniform; site heterogeneity exists because the surface of practical catalyst particles is characterized by terraces of different crystal structures, steps, edges, additives, impurities, and defects. Therefore, it is required to enable MC simulations for such systems in order to derive technical meaningful rates and give insight into geometric and communication effects.

Prior attempts have been made to perform MC simulations on nanoparticles. One approach is to regard a single lattice without periodic boundary conditions as particle and describe the facets as different regions^[19-21]. Another simulation uses three-dimensional particles, which can vary their height to mimic shape transformation. These models use a single lattice with additional information about the particle height for each adsorption place^[22]. Both models neglect the nature of different facets regarding their neighborhood, because they are limited to one lattice type and cannot represent the different neighborhoods of combinations like fcc(111) and fcc(100)-faces. A hybrid approach between a lattice and off-lattice method can overcome these limitations. The facets of the catalyst particle and the support are each described by a lattice, which are linked along their edges (Fig. 2). Since such models lead to a high number of different processes, it is favorable to have a general implementation, which is not restricted to a specific mechanism and allows different particle shapes.

For this, an abstract view on kinetic Monte Carlo simulations has been developed^[23]: Surface processes which occur in catalytic processes as adsorption, desorption, diffusion, and reaction

can be seen as an exchange of patterns. One pattern is describing the positions of the reactants on the surface before the process – the reactant pattern - and another one the position of products after the process – the product pattern (Fig. 1a)).

Lateral interactions can be incorporated into this abstract view as well. From the modeling point of view one distinguishes between hard sphere and soft interactions. Hard sphere interactions are very strong lateral interactions, in which the adsorbed species behave as hard spheres and exclude neighboring places from being occupied. This can be incorporated into the reactant pattern (Fig. 1b)). Soft interactions are of lower energy and cannot be treated as hard sphere interactions. They occur as pairwise interactions but can also be of many species interactions, if detailed cluster expansions are used. One interaction describes how specific neighboring adsorbates influence the activation energy barrier. These interactions can be derived from lattice gas Hamiltonians for the initial state and the transition state. Interactions between the species, which the reactant pattern requires in order to be applied at a specific position, can be incorporated into the fixed activation energy barrier. Interactions between the optional neighboring species are kept in interaction energy tables. Therefore, the energy difference resulting from this place occupied by a specific species is tabulated. Before the process is applied the neighbor dependent interaction energy contributions are added to the fixed activation energy. This works only for pairwise interactions; many species interactions are treated separately.

The surface model assigns each place an occupation and allows the determination of neighboring places. In general, places are not regularly distributed and the surface has to be modeled as a graph, with places as nodes and edges to neighboring places. Places on crystal surfaces obey a translational symmetry, which can be used to systematically enumerate the unit cells and places in each cell. In single lattice codes, the surface can be represented by a

three-dimensional array of integers, i.e. two spatial dimensions and one dimension to account for different lattice places in each unit cell. The extension to structured surfaces uses the same model for each facet. Each place is then described by a lattice id, two spatial coordinates and a place id. Within each facet the neighboring places can be determined via the neighborhood of unit cells. Across the facets neighboring unit cells are connected by links (Fig. 2a)).

This surface model of connected lattices allows an extension of the concept of pattern exchanges to a nanoparticle surface model. A process description has a reactant pattern and a product pattern, which are specific parts of the surface model. Within each facet the processes are described as before (see Fig. 2b)). Processes spanning several facets exhibit more complex reactant and product pattern parts, since they include the links as subsets of the surface model, as well (Fig. 2c)).

Despite this complexity, all described MC algorithms stay applicable, because the following basic procedures are executable for complex processes: Check if a reactant pattern matches the occupation of the surface at a specific position, perform a process at a specific position, i.e. copying of the product pattern to the surface and calculation of the interaction energy.

Single lattice codes apply the pattern at a specific position of the lattice and iterate over the array in order to compare the pattern with the surface. Every pattern has an origin, for which a specific position of the lattice, the application point, indicates where the pattern is applied to the surface. For processes spanning different facets the complete reactant pattern has only one global origin and each pattern part has a local origin. The global application point defines the local application point of only one pattern part directly. The other local application points have to be determined via a depth search over the graph setup by the surface links (Fig. 3).

After the performance of a product pattern, the algorithm VSSM requires an update of the list of possible reactions. An update step has to match the reactant pattern at and around the application point. Since many processes are not even on the same facet or since the product pattern of the step before is contradictory to possible reactant patterns, a list of candidate reactions for each product pattern can be generated to limit the number of process candidates which have to be tested.

If duplicate facets occur within the model, which vary in their shape, but describe the same processes, further optimization is possible. Duplicate facets can be modeled by one single crystal lattice with unused places separating them from each other. This procedure saves the effort to describe the processes for each facet again. The gap of unused places between the mapped facets is determined by the maximal size of reactant pattern for these facets.

Since no complete set of rates is available for a supported nanoparticle, rates for the facets for single crystal surfaces have been taken from literature. The aim of these examples is not to show a well elaborated set of processes, but rather to show the capabilities and limits of the presented methods.

The shape of Pd-particles has been resolved with STM for some support materials^[24-26], even though the (100)-facets have not been resolved in atomic resolution. Despite this, CO-oxidation on Pd-particles marks a well examined system. However, the form of the particles has not been determined under reaction conditions. Therefore, it is assumed in this example, that the form is in accordance to the STM measurements and keeps its shape under reaction conditions. It was transferred to a MC model of a single particle without a support description and to two supported particles (Fig. 4). The system has been described by a MC simulation before^[27]. A MC model for the processes on Pd(100)-crystal surfaces was derived from TPD

experiments^[28]. Whereas for Pd(111)-crystal surfaces process rate values have been taken from simulations^[29-31].

3.3 Reaction rates derived from MC simulations

As for single crystal surfaces, rate models for mean-field calculations can be derived from MC simulations. For a given set of gas phase concentrations and temperature, the surface reaction rate can be derived by averaging over a system in equilibrium or periodic fluctuations (Fig. 5) yielding coefficients for Equations 4.2^[32, 33]. The surface reaction rate can now be directly related to the local conditions in the technical system. Since nanoparticles in technical catalyst exhibit strong variations in size and shape, these variations have to be taken into account in the derivation of rates by kMC simulations leading to numerous simulations of individual particles. Knowing those distributions, averaged rates may be determined for a given distribution of nanostructures of the catalyst and external conditions. Today, this approach can only work for exemplarily cases.

Furthermore, since the implementation of MC simulations into reactor simulations are too computer-time consuming in general, a workaround has to be developed to use the results of MC simulations in CFD simulations of technical systems. Potential methods are the establishment of table-look-up strategies or the derivation of rate expressions from the reaction rates computed as function of gas-phase concentration and temperature by MC simulations. In both methods, the individual state of the catalyst still has to be incorporated, because the state depends on the history of the particle that means the transients of the reactor behavior and associated local conditions.

3.4 Particle – support interaction and spill-over

The catalyst particles cannot be considered as isolated particles. They in general communicate with their neighborhood not only via gas-phase processes (desorption, diffusion, and re-adsorption) but also by diffusive transport on the solid surface. The detailed description of support and nanocatalysts presented above leads, in contrast to single crystal surfaces, to heterogeneous surfaces. Therefore, insight into the influence of geometrical and communication effects on the rate as they occur in real catalyst systems can be gained. The analysis of a MC simulation identifies locations of reactions and diffusion intensities. This provides information on the communication effects between the facets as well as between the support and particle in the form of spill-over effects and reverse spill-over effects^[34].

The expansion of the reverse spill-over effect, i.e. the capture zone of each particle, can be derived by a reverse MC analysis or a net diffusion analysis (Fig. 6). A reverse MC analysis rewinds a simulation run and results in the location, where a reactant has adsorbed depending on the particle, where it reactively desorbed. A strong overlapping of capture zone areas leads to a lowering of the reaction rate per particle (Fig. 7).

The net diffusion analysis sums up the diffusion directions for a specific species at each place. The resulting direction points to the particle where this location mainly “*delivers*” its adsorbates to. Mean-field models taking into account nanocatalysts densities on the support may incorporate the capture zone effect.

3.5 Potentials and limitations of MC simulations for derivation of overall reaction rates

The described kinetic Monte Carlo method with multiple lattices shows the feasibility of a detailed description of the surface and the communication with the support despite a large number of processes. The presented analysis in reversing the simulation and following the

diffusion path of each species results in a general usable analysis of communication and spill-over effects. The hybrid manner between on-lattice and off-lattice approaches provides the possibility to locally use an off-lattice description, which may be useful for clusters consisting of a small number of atoms and lacking any local periodicity.

Of course, the main problems of MC simulations still remain, i.e. the identification of a list with a complete set of processes as well as the presence of fast processes lowering the simulation advance in time. In contrast to crystal surfaces, an empirical derivation of process rates has a much higher effort since the experimental results are averaged over statistical distributions of particle size and shape. In the presented examples no rates for processes at edges were available and therefore only diffusion was considered. If reactions at edges are preferred, this will result in a significant error. Therefore, the presented example can only be considered as a starting point for an exact and geometrical complete model. A detailed analysis of the elementary processes and lateral interactions is still necessary.

In order to fully bridge the geometric gap between *ab-initio* crystal surface simulations and real catalytic surfaces, further development is needed. Several problems have to be solved, which is the connection to the support, the exact description of the impingement rate on and near particles, the account for surface oxidations, and the reshaping of particles during catalysis.

In the presented method, the connection to the support requires a commensurable lattice between support and particle, otherwise the model results in a rather large number of different processes across the links. The latter might be avoided by using an interatomic potential^[35] for the interactions rather than discrete interactions as in LGH. Furthermore the support can

induce strain into the particle which destroys the local periodicity of the facet which is exploited in the given model^[36].

Reshaping of supported nanoparticles has been observed for systems like Rh^[37] and Cu^[38] and opposes towards MC a similar problem as surface oxidations. Simulation of these processes can be made available by stacking several two dimensional lattices, linking three dimensional lattices or switching to a completely three dimensional particle model.

So far the impingement rate for adsorption from kinetic gas theory used in MC simulations is based on the assumption of a free half space above the surface. This assumption is not given for facets and supports, because the reflection-adsorption-ratio and desorption from other surface parts have to be accounted for and are coverage dependent. A possible way to further investigate this is the coupling of the described MC Simulation to molecular dynamics simulations^[39].

As mentioned above, the direct coupling of MC simulations with continuum mechanics simulation is in general not tractable due to computational efforts, at least for most of the technically relevant systems. However, there are a few valuable exceptions. In catalytic combustion, Kissel-Osterrieder et al.^[40] coupled a real time-dependent MC simulation with the surrounding stagnation-point flow field to study the ignition of CO oxidation on Pt and compared with simulations using the mean-field approximation. The same flow configuration was recently used by Matera and Reuter^[41] similar system to study transport limitations and bistability of CO oxidation at RuO₂(110) single crystal surface. They revealed that the coupling of gas-phase transport and surface kinetics leads to an additional complexity, which needs to be accounted for in the interpretation of dedicated in-situ experiments. Hence, the coupling of MC and CFD seems to be of great interest for an atomic-scale understanding of

the function of heterogeneous catalysts used in surface science experiments at technologically relevant gas-phase conditions. While surface science was used to operate the lab reactors at conditions (low pressure, controlled temperature) where mass and heat transfer do not matter, the efforts for bridging the pressure gap calls for more sophisticated computational tools for the interpretation of the measured data.

It is worth to mention that Kolobov et al. ^[42] recently coupled atomistic and continuum models for multi-scale simulations of gas flows by combinations of MC and CFD as well as by combinations of direct Boltzmann solvers with kinetic CFD schemes; the codes were applied to study catalytic growth of vertically aligned carbon nanotubes.

4 Models applicable for numerical simulation of technical catalytic reactors

Since the rate of catalytic reactions is very specific to the catalyst formulation, global rate expressions have been used for many years ^[1, 43, 44]. The reaction rate has often been based on catalyst mass, catalyst volume, reactor volume, or catalyst external surface area. The implementation of this *macrokinetics* approach is straightforward; the reaction rate can easily be expressed by any arbitrary function of gas-phase concentrations and temperature at the catalysts surface calculated at any computational cell containing either catalytically active particles or walls. It is evident that this approach cannot account for the complex variety of phenomena of catalysis and that the rate parameters must be evaluated experimentally for each new catalyst and various external conditions.

The direct computation of surface reaction rates from the molecular situation as discussed above and, in more detail, throughout Chapters 1, 2, and 3 of this book, leads more and more to a comprehensive description, at least for idealized systems. However, DFT, MD, and MC simulations cannot be implemented in complex flow field simulations of technical relevant

systems due to missing algorithms and, more importantly, due to the immense amount of computational time needed. Treating the catalytic system as a *black box* is not the alternative, the knowledge gained from experimental and theoretical surface science studies should be implemented in the chemical models used in the reaction engineering simulation. A tractable approach was proposed for the treatment of surface chemistry in reactive flows in the early 1990ies^[45-47], when the rate equations known from modeling homogeneous reactions systems were adapted to model heterogeneous reactions. This approach was then first computationally realized in the SURFACE CHEMKIN^[48] module of the CHEMKIN^[49, 50] software package; later other packages such as CANTERA^[51] and DETCHEM^[52] as well as many of the commercially available multi-purpose CFD codes adopted this methodology or directly implemented those modules. In the remainder of this section, this concept currently being state of the art in modeling of catalytic reactors will be discussed.

4.1 Mean field approximation and reaction kinetics

The mean field approximation is related to the size of the computational cell in the flow field simulation, assuming that the local state of the active surface can be represented by mean values for this cell. Hence, this model assumes randomly distributed adsorbates on the surface, which is viewed as being uniform (Fig. 9). The state of the catalytic surface is described by the temperature T and a set of surface coverages θ_i , that is the fraction of the surface covered with surface species i . The surface temperature and the coverage depend on time and the macroscopic position in the reactor, but are averaged over microscopic local fluctuations. Under those assumptions a chemical reaction can be defined in analogy to Eq. (2.1) by



The difference is that now the A_i denote not only gas-phase species (e.g., H_2) but also surface species (e.g., $H(s)$) and bulk species (e.g., $H(b)$). The N_s surface species are those that are adsorbed on the top mono-atomic layer of the catalytic particle while the N_b bulk species are those found in the inner solid catalyst.

Steric effects of adsorbed species and various configurations, e.g., the type of the chemical bonds between adsorbate and solid, can be taken into account using the following concept: The surface structure is associated with a surface site density Γ which describes the maximum number of species that can adsorb on a unit surface area, given, e.g., in mol m^{-2} . Then each surface species is associated with a coordination number σ_i describing the number of surface sites which are covered by this species. Under the assumptions made, a multi-step (quasi-elementary) reaction mechanism can be set up. The local chemical source term, R_i^{het} , needed in the CFD simulation of the technical reactor is then derived from the molar net production rate \dot{s}_i by

$$R_i^{\text{het}} = \dot{s}_i M_i = M_i \sum_{k=1}^{K_s} \nu_{ik} k_{f_k} \prod_{j=1}^{N_g + N_s + N_b} c_j^{\nu_{jk}}. \quad (4.2)$$

Here, K_s is the number of surface reactions, c_i are the species concentrations, which are given, e.g., in mol m^{-2} for the N_s adsorbed species and in, e.g., mol m^{-3} for the N_g and N_b gaseous and bulk species. According to Eq. (4.2) and the relation $\Theta_i = c_i \sigma_i \Gamma^{-1}$, the variations of surface coverages follow

$$\frac{\partial \Theta_i}{\partial t} = \frac{\dot{s}_i \sigma_i}{\Gamma}. \quad (4.3)$$

Since the reactor temperature and concentrations of gaseous species depend on the local position in the reactor, the set of surface coverages also varies with position. However, no lateral interaction of the surface species between different locations on the catalytic surface is

modeled. This assumption is justified by the fact that the computational cells in reactor simulations are usually much larger than the range of lateral interactions of the surface processes. In each of these cells, the state of the surface is characterized by mean values (mean-field approximation). The set of differential equations (4.3) has to be solved simultaneously with flow field equations for every computational cell containing catalytic material. At steady state, the left sides of Eqs. (4.3) become zero, and a set of algebraic equations has to be solved. The time scales to reach the steady state of Eqs. (4.3) are commonly much shorter than the time scales of significant variations of species concentrations and temperature in the fluid. Therefore, a quasi-steady state assumption with vanishing left sides of Eqs. (4.3) is frequently justified even for transient reactor operation. For fast transients, usually on the order of $<10^{-4}$ s, this assumption breaks down and the straight implementation of this procedure into CFD simulations becomes more sophisticated^[53, 54].

The binding states of adsorption of all species vary with the surface coverage. This additional coverage dependence is modeled in the expression for the rate coefficient k_{f_k} in Eq. (4.2) by two additional parameters, μ_{i_k} and ε_{i_k} ^[47, 48, 55]:

$$k_{f_k} = A_k T^{\beta_k} \exp\left[\frac{-E_{a_k}}{RT}\right] \prod_{i=1}^{N_s} \Theta_i^{\mu_{i_k}} \exp\left[\frac{\varepsilon_{i_k} \Theta_i}{RT}\right] \quad (4.4)$$

For adsorption reactions sticking coefficients are commonly used, which can be converted to conventional rate coefficients^[47] by

$$k_{f_k}^{\text{ads}} = \frac{S_i^0}{\Gamma^\tau} \sqrt{\frac{RT}{2\pi M_i}} \quad , \text{ where } \tau = \sum_{j=1}^{N_s} \nu'_{jk} \quad (4.5)$$

S_i^0 is the initial (uncovered surface) sticking coefficient. At high sticking coefficients a correction needs to be applied^[47].

4.2 Thermodynamic consistency

A crucial issue with many of the mechanisms published is thermodynamic consistency. Even though most of the mechanisms lead to consistent enthalpy diagrams, many are not consistent regarding the entropy change in the overall reaction due to missing knowledge on the transition states of the individual reactions and therefore on the pre-exponentials in the rate equations. Lately, optimization procedures enforcing overall thermodynamic consistency have been applied to overcome this problem^[56, 57]; here we present one^[57] of these approaches.

The equilibrium of a reversible chemical reaction,



is completely defined by the thermodynamic properties of the participating species. Expressed in terms of the equilibrium constant, K_{pk} , the equilibrium activities, a_i^{eq} , obey the equation

$$K_{pk} = \prod_i (a_i^{\text{eq}})^{\nu_{ik}} = \exp\left(-\frac{\Delta_k G^0}{RT}\right). \quad (4.7)$$

The change of free enthalpy at normal pressure p^0 is

$$\Delta_k G^0 = \sum_i \nu_{ik} G_i^0(T) . \quad (4.8)$$

In case of gases, the activities can be approximated by their partial pressures $a_i = p_i/p^0$, and in case of surface species by their coverages $a_i = \Theta_i$. When the dependence of the heat capacities on temperature is given by a forth-order polynomial^[45] and standard enthalpies and entropies of formation, then the standard free enthalpies can be expressed in terms of seven coefficients, $a_{0,i}, \dots, a_{6,i}$:

$$G_i^0(T) = a_{0,i} + a_{1,i}T + a_{2,i}T^2 + a_{3,i}T^3 + a_{4,i}T^4 + a_{5,i}T^5 + a_{6,i}T \ln T . \quad (4.9)$$

In order to predict the correct equilibrium, the rate coefficients for the forward and the reverse reaction must obey the equation

$$\frac{k_{f_k}}{k_{r_k}} = K_{pk} \cdot \prod_i (c_i^0)^{\nu_{ik}} . \quad (4.10)$$

The c_i^0 are reference concentrations at normal pressure, i.e. $c_i^0 = p^0/RT$ for gas-phase species and $c_i^0 = \Gamma/\sigma_i$ for surface species.

However, one problem in setting up a reaction mechanism is the difficulty to define the thermodynamic data for intermediate surface species. Therefore, Eq. (4.10) cannot be used to calculate the rate coefficient of the reverse reaction. The forward and the reverse reaction are then defined separately with their own rate laws. Nevertheless, these rates cannot be chosen independently.

Therefore, the following method is proposed^[57]: Assume an initial guess for a surface reaction mechanism. The rate coefficients for forward and reverse reactions may have been adjusted separately. Suppose that the thermodynamic data for species $1 \dots N_u$ are unknown. For each pair of reversible reactions we can calculate an equilibrium constant using Eq. (4.10) and, according to Eq. (4.7), its logarithm yields the change of free enthalpy. (Note: coverage dependent activation energies are not considered at this stage.) Separation of the known and the unknown variables in Eq. (4.8) leads to

$$\Delta_k G^0 = \sum_{i=1}^{N_u} \nu_{ik} \tilde{G}_i^0(T) + \sum_{i=N_u+1}^N \nu_{ik} G_i^0(T), \quad (4.11)$$

that is a linear equation system for the unknown free enthalpies \tilde{G}_i^0 . Since most species are involved in more than one reaction, this system is usually over-determined. Inserting Eq. (4.9)

for several temperatures, T_j gives a system of linear equations in the unknown coefficients

$\tilde{a}_{l,i}$:

$$\sum_{i=1}^{N_u} \sum_{l=0}^6 \nu_{ik} t_{lj} \tilde{a}_{l,i} = g_{kj} \quad \text{for all } k \text{ and } j, \quad (4.12)$$

where the following abbreviations have been used

$$g_{kj} = \Delta_k G^0(T_j) - \sum_{i=N_u+1}^N \nu_{ik} G_i^0(T_j) \quad \text{and} \quad (4.13)$$

$$t_{lj} = \begin{cases} T_j^l & \text{if } l < 6 \\ T_j \ln T_j & \text{if } l = 6 \end{cases} \quad (4.14)$$

An “optimal” set of parameters $\tilde{a}_{l,i}$ is determined by a weighted least-square approximation.

The weights can be chosen individually for each pair of reactions according to a sensitivity analysis of the reaction mechanism. This guarantees that the equilibrium of crucial reaction steps will be shifted less than others after adjustment.

The newly adjusted thermodynamic coefficients are then used to calculate the change of free enthalpy for each reaction (4.11), the equilibrium constant (4.7), and the rate coefficient of the reverse reaction (4.10). In case the reverse reaction shall be expressed in terms of Arrhenius coefficients, another least square approximation using the rate constants at the discrete temperatures, T_j , is performed.

Since writing of surface reaction mechanisms as pairs of irreversible reactions is often more convenient, this procedure has to be repeated during mechanism development after modification of rate coefficients belonging to any of these pairs. Figure 9 illustrates the algorithm. The difference between this method and the scheme proposed by Mhadeshwar et al.^[56] is the fact that in the procedure described there is no need to select a linearly

independent set of reactions. Instead of distinguishing reactions between linear base and linear combinations, all reactions are treated equally by solving the same linear problem using a least-square fit.

Exemplarily, Table 2 lists a surface reaction mechanism for steam-reforming over Ni-based catalysts, which has been adjusted to be thermodynamically consistent according to this procedure. The mechanism has successfully been used to model steam reforming of methane over Ni/Al₂O₃ catalysts^[57] and thermo-catalytic conversion of partially pre-reformed methane in solid-oxide fuel cells (SOFC)^[58, 59].

4.3 Practicable method for development of multi-step surface reaction mechanisms

The development of a reliable surface reaction mechanism is a complex process following the scheme given in Fig. 10. A tentative reaction mechanism can be proposed based on experimental surface science studies, on analogy to gas-phase kinetics and organo-metallic compounds, and on theoretical studies, increasingly including DFT calculations^[60, 61], and in the future also MD and MC simulations as discussed above^[32, 34]. This mechanism should include all possible paths for the formation of the chemical species under consideration in order to be “elementary-like” and thus applicable over a wide range of conditions. The mechanism idea then needs to be evaluated by numerous experimentally derived data, which are compared with theoretical predictions based on the mechanism. Here, the simulations of the laboratory reactors require appropriate models for all significant processes in order to evaluate the intrinsic kinetics.

A key step in improving detailed reaction mechanisms is the application of sensitivity analyses, which leads to the crucial steps in the mechanism for which refined kinetic

experiments and data may be needed.^[62] This technique has been applied in understanding homogeneous combustion processes for decades^[12]. A similar approach called *degree of rate control* has been introduced by Campbell et al.^[63]. Sensitivity analysis allows for an identification of the individual reaction steps that are most influential to the system. Several methods can be used in order to calculate the sensitivity of the solution, i.e., the time behavior of the different species profiles with respect to the rate coefficients. The most straight-forward way is to simply run a calculation and then rerun it after changing the parameters successively. Although being very simple, this approach has the disadvantage of requiring a large amount of computational power for the n_p parameters for which sensitivities have to be calculated. Furthermore, here the errors result from the fact that the parameters have to be changed by a finite amount, which is sufficiently large to observe an effect on the overall solution, which is not superimposed by discretization errors.

A more elegant way is the direct solution of the sensitivity equations together with the solution of the system equations^[64]. In order to derive the governing equations for the sensitivity coefficients, we consider the differential - algebraic equation systems describing the chemical reactor under consideration:

$$\mathbf{B} \frac{\partial \vec{y}}{\partial t} = \vec{F}(\vec{y}, t; \vec{p}), \quad (4.15)$$

where \vec{y} is the n -dimensional vector of the dependent variables (species partial pressures, temperature, coverages, ...) and \vec{p} the vector of the n_p system variables (rate parameters, transport coefficients,...); \vec{F} is the vector function of these variables. The sensitivity coefficients are defined as

$$s_{ij} = \frac{\partial y_i}{\partial p_j}. \quad (4.16)$$

Partial differentiation of Eq. (4.15) with respect to the n_p parameters p_j leads to

$$\overline{\mathbf{B}} \frac{\partial \overline{\mathbf{S}}(t)}{\partial t} = \overline{\mathbf{F}}_y \overline{\mathbf{S}}(t) + \overline{\mathbf{F}}_p(t), \quad (4.17)$$

where $\overline{\mathbf{S}}$ is the matrix of the time-dependent sensitivity coefficients, $\overline{\mathbf{F}}_y$ is the Jacobian, $\partial F_i / \partial y_j$, and $\overline{\mathbf{F}}_p$ is the matrix of the derivation of \overline{F} with respect to the system parameters \overline{p} , i.e., $\partial F_i / \partial p_j$. In case of rate coefficients k_j as system parameters, we get

$$s_{ij} = \frac{\partial y_i}{\partial \ln k_j}. \quad (4.18)$$

Consequently, the macroscopic variable y_i will be changed by 1% times s_{ij} for a change of k_j by 1%.^[64]

Exemplarily, Fig. 11 shows the normalized sensitivity coefficients concerning the sensitivity of the vacancies (uncovered adsorption sites) on rate coefficients of surface reactions immediately before catalytic ignition of methane oxidation in a stagnation-point flow onto a platinum foil^[53]. The decisive parameters for ignition are the rates of adsorption and desorption of oxygen on the surface, i.e., the adsorption-desorption equilibrium of oxygen on Pt, which becomes clear studying the surface coverages as shown in Figure 12. Oxygen coverage inhibits methane adsorption before ignition.

The application of sensitivity analysis is also a powerful tool in identifying the rate limiting steps in a detailed chemical reaction mechanism, which then can be used to set up even simpler rate expressions such as used in the LHHW model.

The coupling of several complex models introduces a large number of parameters into the simulations. For instance, detailed reaction schemes may have hundreds of kinetic parameters, each value associated with a certain inaccuracy. Hence, agreement between predicted and

experimentally observed overall conversion and selectivity alone is not sufficient to evaluate individual sub models. Consequently, once established mechanisms require continuous evaluation. Eventually, reaction mechanisms are rather falsified by applying them; they can never be verified! One can never be sure not to have missed certain reaction pathways. Hence, the practical development and testing shall include large sets of experimental data at a wide variety of external conditions (temperature, chemical composition, contact time). The use of experimental data for the same chemical system but in different flow configurations limits the risk of having transport effects, primarily internal diffusion, included in the intrinsic kinetics. The use of experimental data of different groups helps in a similar way.

Recently, a new platform – available on the web under www.detchem.com – has been established to assist in development of surface reaction mechanisms. On this platform, experimental data and the corresponding computational tools (flow models) for their numerical simulation are given. The user can choose a set of *real* and *numerical* experiments for a certain chemical system, e.g. NO oxidation over Pt, and a corresponding reaction mechanism, which can be modified, and let the underlying computers do the simulation. As results comparison of experimental and numerical predicted conversion, selectivities, profiles or any other relevant variables are presented. Using this computational tool, one can easily test a new or modified kinetic scheme versus a large set of experimental data points. This procedure will not only boost the development of reaction mechanisms but also help to indentify experimental situations (conditions, support effects, false measurements) that need further considerations.

Time and locally resolved profiles provide a more stringent test for model evaluation. Useful data arise from spatial and temporal species profiles by in situ, non-invasive methods such as Raman and laser induced fluorescence (LIF) spectroscopy. For instance, an optically

accessible catalytic channel reactor can be used to evaluate models for heterogeneous and homogeneous chemistry as well as transport by the simultaneous detection of stable species by Raman measurements and OH radicals by Planar laser-induced fluorescence (PLIF) ^[65, 66]. For instance, the reliability of different heterogeneous and homogeneous reaction schemes proposed in literature was investigated by comparison of the experimentally derived ignition distances with numerical elliptic two-dimensional simulations of the flow field using combinations of a variety of schemes ^[67-70]. While some models perform well, others lead to quite inaccurate predictions. Model evaluation is discussed in more detail in Chapter 6 of this book.

Since the early nineties, many groups have developed surface reaction mechanisms following the mean-field approximation. Oxidation reactions over noble metals in particular have been modeled extensively such as of hydrogen ^[46, 71-76], CO ^[77-79], and methane ^[53, 80-84] and ethane ^[7, 11, 85, 86] over Pt, formation of synthesis gas over Rh ^[84, 87]. Lately, mechanisms have been established for more complex reaction systems, for instance, three-way catalysts ^[88] or Chemical Vapor Deposition (CVD) reactors for the formation of diamond ^[89, 90], silica ^[91], and nanotubes ^[92]. Table 4 lists a selection of heterogeneous reaction mechanisms following the concept of the mean-field approximation; the list is far from being complete.

4.4 Potentials and limitations of the mean-field approximation

Catalytic surfaces are certainly non-uniform; site heterogeneity exists because the surface of practical catalyst particles is characterized by terraces of different crystal structures, steps, edges, additives, impurities, and defects. In the mean-field approximation, the site heterogeneity is averaged out by mean rate coefficients. If the distribution of the different types of adsorption sites and the reaction kinetics on those sites are known, this concept can easily be used to set up a reaction mechanism, which consists of several sub-mechanisms for

the different surface structures ^[48]. This concept was applied in the framework of a two-adsorption site model for the simulation of CO combustion on polycrystalline Pt ^[93]. The site heterogeneity can be described by the probability that an arbitrary site is characterized by the associated reaction kinetics. In the models discussed so far, this probability function is a sum over a finite number of surface structures; however, continuous functions are used in literature, as well ^[2]. Here, the problem is the limited knowledge of the distribution of the different types of surface patches and the kinetics on these patches, again.

Effects resulting from lateral interactions of the adsorbates are inherently more difficult to treat. In the mean-field approximation they are either neglected or incorporated by mean rate coefficients. If the specific adsorbate-adsorbate interactions are understood quantitatively, a Monte Carlo (MC) simulation of the surface chemistry can be carried out as discussed above.

The amount of catalyst in a technical system is generally determined rather by the active catalytic surface area than the total amount of catalysts used, that means the dispersion of the catalyst matters. The active catalytic surface area can be experimentally determined by chemisorption studies using CO or H₂. Since the molar surface reaction rate, Eq. 4.2, is given per catalyst surface area (mol (m² s)⁻¹), the active catalytic surface area serves as scaling parameter to compute the chemical source term due to heterogeneous reactions per volumetric or surface element of the reactor. Recently, it was shown that the active catalytic surface area can also be used to describe the change of reaction rates with varying catalyst loading as well as due to hydrothermal ageing ^[94, 95].

Another crucial issue of MF kinetics is the origin of the kinetic data, in particular the activation energies. Since data from DFT simulation become more and more available and the commercial codes are easy to use even for non-experts, DFT derived data have found their

way into reaction engineering modeling. Two concerns have to be mentioned. First, not all DFT data published are trust-worthy; the assumptions used in the simulation, such as size of the unit cell, effect of co-adsorbates, or choice of the functional, are often not justified. Furthermore, the uncertainties of the data computed may be too large for a meaningful implementation into a complex reaction mechanism. The second point here lies in the intrinsic assumptions of the mean-field approximation, which is that the individual morphology and size of the catalyst particle is not taken into account. In particular, the individual kinetics of the general crystal phase is usually not considered, even though it is principally possible. As discussed above and in previous chapters, the molecular processes are rather too complex for an adequate description within the concept of the mean-field approximation. If only one single crystal phase or a certain defect structure determines the overall reaction rate of the catalyst particle, then DFT simulations of these phases and structures may be implemented directly into a mean-field model but often this is not the case. Reuter et al. recently studied this phenomenon in detail^[96] high-lightening the problems that arise when MF simulations are based on first-principal computations only. The averaging over individual microscopic events implies that – in general – the direct use of DFT data in MF simulations is at least questionable. We often found that MF based mechanisms are more reliable when rather based on semi-empirical methods such as UBI-QEP^[97] than on pure DFT data. The right way seems to be to use DFT data in MC simulations and feed the MC computed rates into a kind of rate expression instead of using DFT directly in MF. Unfortunately, the approach from DFT to MC to MF is quite tricky. Therefore, the model of choice in reaction engineering simulations is likely going to remain the MF approach combining knowledge gained from surface science and experiments at technical relevant conditions in a pragmatic way. This approach, which definitely has its deficiencies, has also shown some robustness and reliability and has quite often proven to not only help to understand the complex interactions of heterogeneous

chemical kinetics with mass and heat transport in laboratory reactors but also to support design and optimization of technical catalytic reactors.

5 Simplifying complex kinetic schemes

Even though the previous section discusses a variety of simplifications used in the established reaction mechanisms, these kinetic schemes are sometimes still too complex for direct use in CFD simulations. They introduce an additional highly nonlinear coupling into the governing equations of CFD simulations, which leads to considerable computational efforts, in particular when used in simulations of turbulent flows (e.g., in flow reactors) and in simulations with continuously varying inlet and boundary conditions (e.g., in automobile catalytic converters). The nonlinearity, the large number of chemical species in different phases, and the fact that surface reactions in particular exhibit a large range of time scales make the solution of those equation systems challenging. In particular for transient simulations such as simulations of the behavior of catalytic converters during entire driving cycles^[98], the solution of the system is too CPU time-consuming with current numerical algorithms and computer capacities.

Therefore, many groups use global reaction schemes with kinetic data derived from experimental data such as conversion and selectivity as function of temperature through a pure fitting process using well-established optimization procedures^[99]. Due to the complexity in the chemical processes many additional parameters, e.g., through so-called inhibition terms, have to be introduced to let the model match a large set of experimental data^[94, 100]. Sometimes the number of parameters needed to describe all effects in such global reaction schemes can even exceed the number of parameters used in molecular based multi-step reaction mechanisms (MF approximation).

Consequently, the increase in computing time with an increasing number of species and reactions implemented in the CFD simulation calls for the application of reduction algorithms for large reaction mechanisms. One approach is the extraction of the intrinsic low dimensional manifolds of trajectories in chemical space ^[15], once developed for homogeneous reaction mechanisms but meanwhile also applied for heterogeneous reactions ^[101].

Votsmeier et al. recently developed several alternative strategies to use data-based models in the form of splines, neural networks, and look-up tables in CFD simulations of complex technical reactors^[102, 103]. They demonstrated for instance that pre-computed rate data can be used to enable the numerically efficient implementation of mechanistic kinetics in a reactor model for an automotive ammonia slip catalyst^[103]. The source terms of the gas species are mapped (80,000 data points) as a function of gas composition and temperature to construct a spline interpolation function resulting in a speedup of about two orders of magnitude at an error of less than 1%^[103].

6 Summary and outlook

Today, most of the models for the description of the heterogeneous reaction rates used in reaction engineering computations are based on the mean field approximation, in which the local state of the surface is described by its coverage with adsorbed species averaged on a microscopic scale. The averaging procedure questions the direct use of kinetic data derived from molecular-based surface science experiments and simulations such as density functional theory (DFT). In general, an intermediate step needs to be introduced. The most promising flow of information in this case is from DFT to MC to MF: DFT derived activation energies for reactions and diffusion processes on nanoparticle catalysts are used in Monte Carlo (MC) simulations, which directly provide the local heterogeneous reaction rates as function of gas-phase concentrations, temperature, and state of the catalyst particle (coverage, oxidation state,

size, morphology). These reaction rates can then be implemented into MF models. MD simulations may complete this pathway, coming in between DFT and MC. Although, tremendous progress has recently been made in the efficient and reliable provision of DFT data and their use in MC simulations as well as the implementation of “real catalyst” effects such as spill-over and catalyst-support interaction into the MC techniques, this approach can currently be used for simple and exemplarily cases only. The computational efforts are simply too large.

On the other side, global reaction kinetics with dozens of fitted parameters with little or even “black box” models without any mechanistic insight are still in use in scale-up and design of technical catalytic reactors. Hence, one of the challenges in modeling heterogeneous reaction rates still remaining is the transfer of the knowledge gained in experimental and theoretical surface science into models tractable for numerical simulation of technical catalytic reactors. There is still a large gap to be bridged. Currently the only way seems to be the rather tedious one, collecting all the information from surface science into the mechanistic models that need to be evaluated by experimental studies under technical conditions to come up with (intrinsic) kinetic rate expressions usable in CFD simulations. Alternatively, sophisticated (e.g., neuronal networks) generic, data based models treating the reactor as black box but covering all potential ranges of reactor operation can be applied. However, those models will not allow the exploration of the full optimization potential of the reactor, in particular concerning the optimized interplay between chemical reactions in different phases and mass and heat transfer.

Some of the present major challenges in modeling heterogeneous reactions in technical systems are: catalyst support interactions, spill-over, multi-functional catalysts, operando modifications of the catalyst (oxidation/reduction cycles, storage/regeneration, partial melting

etc.), non-thermally equilibrated nanoparticles, structure sensitivity, aging (agglomeration, coking, oxidation), and implementation of detailed kinetics models into numerical simulation of catalytic reactors, as discussed in the last chapters of the book.

Acknowledgment

The authors would like to thank Y. Dedecek (Karlsruhe Institute of Technology) for editorial corrections of the manuscript. Financial support of our work on modeling heterogeneous catalysis by the German Research Foundation (DFG) and the Helmholtz Association through the Helmholtz Research School Energy-Related Catalysis is gratefully acknowledged.

References

- [1] O. Deutschmann, H. Knözinger, K. Kochloefl, T. Turek, *Heterogeneous Catalysis and Solid Catalysts.*, 7th ed., Wiley-VCH Verlag, Weinheim, **2009**.
- [2] J. A. Dumesic, D. F. Rudd, L. M. Aparicio, J. E. Rekoske, A. A. Trevino, *The Microkinetics of Heterogeneous Catalysis*, American Chemical Society, Washington, DC, **1993**.
- [3] M. Boudart, *Catalysis Letters* **2000**, 65, 1.
- [4] A. Beretta, P. Forzatti, E. Ranzi, *Journal of Catalysis* **1999**, 184, 469.
- [5] A. Beretta, P. Forzatti, *Journal of Catalysis* **2001**, 200, 45.
- [6] A. Beretta, E. Ranzi, P. Forzatti, *Chemical Engineering Science* **2001**, 56, 779.
- [7] D. K. Zerkle, M. D. Allendorf, M. Wolf, O. Deutschmann, *Journal of Catalysis* **2000**, 196, 18.
- [8] R. Subramanian, L. D. Schmidt, *Angewandte Chemie-International Edition* **2005**, 44, 302.
- [9] J. J. Krummenacher, L. D. Schmidt, *Journal of Catalysis* **2004**, 222, 429.
- [10] L. D. Schmidt, J. Siddall, M. Bearden, *American Institute of Chemical Engineering Journal* **2000**, 46, 1492.
- [11] F. Donsi, K. A. Williams, L. D. Schmidt, *Industrial & Engineering Chemistry Research* **2005**, 44, 3453.
- [12] J. Warnatz, R. W. Dibble, U. Maas, *Combustion, Physical and Chemical Fundamentals, Modeling and Simulation, Experiments, Pollutant Formation*, Springer-Verlag, New York, **1996**.
- [13] A. M. Dean, *Journal of Physical Chemistry* **1990**, 94, 1432.
- [14] M. Dente, E. Ranzi, A. G. Goossens, *Computers & Chemical Engineering* **1979**, 3, 61.
- [15] U. Maas, S. Pope, *Combustion and Flame* **1992**, 88, 239.
- [16] R. G. Susnow, A. M. Dean, W. H. Green, P. Peczak, L. Broadbelt, *Journal of Physical Chemistry A* **1997**, 101, 3731.
- [17] A. B. Bortz, M. H. Kalos, J. L. Lebowitz, *Journal of Computational Physics* **1975**, 17, 10.
- [18] J. J. Lukkien, J. P. L. Segers, P. A. J. Hilbers, R. J. Gelten, A. P. J. Jansen, *Physical Review E* **1998**, 58, 2598.
- [19] F. Maillard, M. Eikerling, O. V. Cherstiouk, S. Schreier, E. Savinova, U. Stimming, *Faraday Discussions* **2004**, 125, 357.
- [20] V. P. Zhdanov, B. Kasemo, *Surface Science* **1998**, 405, 27.
- [21] V. P. Zhdanov, B. Kasemo, *Physical Review Letters* **1998**, 81, 2482.
- [22] E. V. Kovalyov, E. D. Resnyanskii, V. I. Elokhin, B. S. Bal'zhinimaev, A. V. Myshlyavtsev, *Physical Chemistry Chemical Physics* **2003**, 5, 784.
- [23] J. P. L. Segers, PhD thesis, Technische Universiteit Eindhoven (Eindhoven), **2000**.
- [24] F. Silly, M. R. Castell, *Physical Review Letters* **2005**, 94, 046103.
- [25] K. H. Hansen, oslash, jrur, T. Worren, S. Stempel, aelig, E. gsgaard, auml, M. umer, H. J. Freund, F. Besenbacher, I. Stensgaard, *Physical Review Letters* **1999**, 83, 4120.
- [26] S. K. Shaikhutdinov, R. Meyer, D. Lahav, auml, M. umer, Kl, uuml, T. ner, H. J. Freund, *Physical Review Letters* **2003**, 91, 076102.
- [27] J. Hoffmann, PhD Thesis thesis, Freie Universität Berlin (Berlin), **2003**.
- [28] D.-J. Liu, J. W. Evans, *The Journal of Chemical Physics* **2006**, 124, 154705.
- [29] K. Honkala, Piril, auml, P., ivi, K. Laasonen, *Physical Review Letters* **2001**, 86, 5942.
- [30] T. Mitsui, M. K. Rose, E. Fomin, D. F. Ogletree, M. Salmeron, *Physical Review Letters* **2005**, 94, 036101.
- [31] M. Lynch, P. Hu, *Surface Science* **2000**, 458, 1.
- [32] L. W. H. Kunz, Diploma thesis, Universität Karlsruhe (TH) (Karlsruhe), **2006**.

- [33] L. W. H. Kunz, O. Deutschmann, *Physical Review B* **2011**, to be submitted.
- [34] L. W. H. Kunz, O. Deutschmann, *Journal of Catalysis* **2011**, to be submitted.
- [35] C. Bos, PhD thesis, Universität Stuttgart (Stuttgart), **2006**.
- [36] J. Meier, J. Schiøtz, P. Liu, J. K. Nørskov, U. Stimming, *Chemical Physics Letters* **2004**, 390, 440.
- [37] P. Nolte, A. Stierle, N. Y. Jin-Phillipp, N. Kasper, T. U. Schulli, H. Dosch, *Science* **2008**, 321, 1654.
- [38] P. L. Hansen, J. B. Wagner, S. Helveg, J. R. Rostrup-Nielsen, B. S. Clausen, H. Topsøe, *Science* **2002**, 295, 2053.
- [39] J. M. Pomeroy, J. Jacobsen, C. C. Hill, B. H. Cooper, J. P. Sethna, *Physical Review B* **2002**, 66, 235412.
- [40] R. Kissel-Osterrieder, F. Behrendt, J. Warnatz, *Proceedings of the Combustion Institute* **1998**, 27, 2267.
- [41] S. Matera, K. Reuter, *Physical Review B* **2010**, 82, 085446.
- [42] V. Kolobov, R. Arslanbekov, A. Vasenkov, in *Computational Science - ICCS 2007, Pt 1, Proceedings, Vol. 4487* (Eds.: Y. Shi, G. D. VanAlbada, J. Dongarra, P. M. A. Sloot), **2007**, pp. 858.
- [43] M. Baerns, H. Hofmann, A. Renken, *Chemische Reaktionstechnik*, Georg Thieme Verlag, Stuttgart, New York, **1992**.
- [44] R. E. Hayes, S. T. Kolaczkowski, *Introduction to Catalytic Combustion*, Gordon and Breach Science Publ., Amsterdam, **1997**.
- [45] M. E. Coltrin, R. J. Kee, F. M. Rupley, *International Journal of Chemical Kinetics* **1991**, 23, 1111.
- [46] J. Warnatz, *Proceedings of the Combustion Institute* **1992**, 24, 553.
- [47] R. J. Kee, M. E. Coltrin, P. Glarborg, *Chemically Reacting Flow*, Wiley-Interscience, **2003**.
- [48] M. E. Coltrin, R. J. Kee, F. M. Rupley, *SURFACE CHEMKIN (Version 4.0): A Fortran Package for Analyzing Heterogeneous Chemical Kinetics at a Solid-Surface - Gas-Phase Interface, SAND91-8003B*, Sandia National Laboratories, **1991**.
- [49] R. J. Kee, F. M. Rupley, J. A. Miller, *CHEMKIN-II: A Fortran Chemical Kinetics Package for the Analysis of Gas-Phase Chemical Kinetics, SAND89-8009*, Sandia National Laboratories, **1998**.
- [50] R. J. Kee, F. M. Rupley, J. A. Miller, M. E. Coltrin, J. F. Grcar, E. Meeks, H. K. Moffat, A. E. Lutz, G. Dixon-Lewis, M. D. Smooke, J. Warnatz, G. H. Evans, R. S. Larson, R. E. Mitchell, L. R. Petzold, W. C. Reynolds, M. Caracotsios, W. E. Stewart, P. Glarborg, C. Wang, O. Adigun, *CHEMKIN*, 3.6 ed., Reaction Design, Inc., www.chemkin.com, San Diego, **2000**.
- [51] D. G. Goodwin, *CANTERA. An open-source, extensible software suite for CVD process simulation*, www.cantera.org, **2003**.
- [52] O. Deutschmann, S. Tischer, C. Correa, D. Chatterjee, S. Kleditzsch, V. M. Janardhanan, *DETCHEM software package*, 2.0 ed., www.detchem.com, Karlsruhe, **2004**.
- [53] O. Deutschmann, R. Schmidt, F. Behrendt, J. Warnatz, *Proceedings of the Combustion Institute* **1996**, 26, 1747.
- [54] L. L. Raja, R. J. Kee, L. R. Petzold, *Proceedings of the Combustion Institute* **1998**, 27, 2249.
- [55] O. Deutschmann, in *Handbook of Heterogeneous Catalysis, 2nd Ed.* (Ed.: H. K. G. Ertl, F. Schüth, J. Weitkamp), Wiley-VCH, **2007**.
- [56] A. B. Mhadeshwar, H. Wang, D. G. Vlachos, *Journal of Physical Chemistry B* **2003**, 107, 12721.

- [57] L. Maier, B. Schädel, K. Herrera Delgado, S. Tischer, O. Deutschmann, *Topics in Catalysis* **2011**, *submitted*.
- [58] E. S. Hecht, G. K. Gupta, H. Y. Zhu, A. M. Dean, R. J. Kee, L. Maier, O. Deutschmann, *Applied Catalysis a-General* **2005**, *295*, 40.
- [59] V. M. Janardhanan, O. Deutschmann, *Journal of Power Sources* **2006**, *162*, 1192.
- [60] O. R. Inderwildi, D. Lebiez, O. Deutschmann, J. Warnatz, *Journal of Chemical Physics* **2005**, *122*.
- [61] A. Heyden, B. Peters, A. T. Bell, F. J. Keil, *Journal of Physical Chemistry B* **2005**, *109*, 4801.
- [62] F. Behrendt, O. Deutschmann, U. Maas, J. Warnatz, *Journal of Vacuum Science & Technology a-Vacuum Surfaces and Films* **1995**, *13*, 1373.
- [63] C. T. Campbell, *Journal of Catalysis* **2001**, *204*, 520.
- [64] O. Deutschmann, Dissertation thesis, Universität Heidelberg (Heidelberg), **1996**.
- [65] C. Appel, J. Mantzaras, R. Schaeren, R. Bombach, B. Kaeppli, A. Inauen, *Proceedings of the Combustion Institute* **2003**, *29*, 1031.
- [66] M. Reinke, J. Mantzaras, R. Schaeren, R. Bombach, W. Kreutner, A. Inauen, *Proceedings of the Combustion Institute* **2002**, *29*, 1021.
- [67] U. Dogwiler, P. Benz, J. Mantzaras, *Combustion and Flame* **1999**, *116*, 243.
- [68] J. Mantzaras, C. Appel, P. Benz, *Proceedings of the Combustion Institute* **2000**, *28*, 1349.
- [69] J. Mantzaras, C. Appel, *Combustion and Flame* **2002**, *130*, 336.
- [70] M. Reinke, J. Mantzaras, R. Schaeren, R. Bombach, A. Inauen, S. Schenker, *Combustion and Flame* **2004**, *136*, 217.
- [71] W. R. Williams, C. M. Marks, L. D. Schmidt, *Journal of Physical Chemistry* **1992**, *96*, 5922.
- [72] B. Helling, B. Kasemo, V. P. Zhdanov, *Journal of Catalysis* **1991**, *132*, 210.
- [73] M. Rinnemo, O. Deutschmann, F. Behrendt, B. Kasemo, *Combustion and Flame* **1997**, *111*, 312.
- [74] G. Vesper, *Chemical Engineering Science* **2001**, *56*, 1265.
- [75] P.-A. Bui, D. G. Vlachos, P. R. Westmoreland, *Industrial & Engineering Chemistry Research* **1997**, *36*, 2558.
- [76] J. C. G. Andrae, P. H. Björnbo, *American Institute of Chemical Engineering Journal* **2000**, *46*, 1454.
- [77] J. Mai, W. von Niessen, A. Blumen, *Journal of Chemical Physics* **1990**, *93*, 3685.
- [78] V. P. Zhdanov, B. Kasemo, *Applied Surface Science* **1994**, *74*, 147.
- [79] P. Aghalayam, Y. K. Park, D. G. Vlachos, *Proceedings of the Combustion Institute* **2000**, *28*, 1331.
- [80] G. Vesper, J. Frauhammer, L. D. Schmidt, G. Eigenberger, in *Studies in Surface Science and Catalysis 109*, **1997**, pp. 273.
- [81] P.-A. Bui, D. G. Vlachos, P. R. Westmoreland, *Surface Science* **1997**, *386*, L1029.
- [82] U. Dogwiler, P. Benz, J. Mantzaras, *Combustion and Flame* **1999**, *116*, 243.
- [83] P. Aghalayam, Y. K. Park, N. Fernandes, V. Papavassiliou, A. B. Mhadeshwar, D. G. Vlachos, *Journal of Catalysis* **2003**, *213*, 23.
- [84] D. A. Hickman, L. D. Schmidt, *American Institute of Chemical Engineering Journal* **1993**, *39*, 1164.
- [85] M. Huff, L. D. Schmidt, *Journal of Physical Chemistry* **1993**, *97*, 11815.
- [86] M. C. Huff, I. P. Androulakis, J. H. Sinfelt, S. C. Reyes, *Journal of Catalysis* **2000**, *191*, 46.
- [87] R. Schwiedernoch, S. Tischer, C. Correa, O. Deutschmann, *Chemical Engineering Science* **2003**, *58*, 633.
- [88] D. Chatterjee, O. Deutschmann, J. Warnatz, *Faraday Discussions* **2001**, *119*, 371.

- [89] B. Ruf, F. Behrendt, O. Deutschmann, J. Warnatz, *Surface Science* **1996**, 352, 602.
- [90] S. J. Harris, D. G. Goodwin, *Journal of Physical Chemistry* **1993**, 97, 23.
- [91] S. Romet, M. F. Couturier, T. K. Whidden, *Journal of the Electrochemical Society* **2001**, 148, G82.
- [92] C. D. Scott, A. Povitsky, C. Dateo, T. Gokcen, P. A. Willis, R. E. Smalley, *Journal of Nanoscience and Nanotechnology* **2003**, 3, 63.
- [93] R. Kissel-Osterrieder, F. Behrendt, J. Warnatz, U. Metka, H. R. Volpp, J. Wolfrum, *Proceedings of the Combustion Institute* **2000**, 28, 1341.
- [94] K. Hauff, U. Tuttlies, G. Eigenberger, U. Nieken, *Applied Catalysis B-Environmental*, **100**, 10.
- [95] W. Boll, S. Tischer, O. Deutschmann, *Industrial & Engineering Chemistry Research* **2010**, 49, 10303.
- [96] B. Temel, H. Meskine, K. Reuter, M. Scheffler, H. Metiu, *Journal of Chemical Physics* **2007**, 126, 12.
- [97] E. Shustorovich, H. Sellers, *Surface Science Reports* **1998**, 31, 1.
- [98] J. Braun, T. Hauber, H. Többen, J. Windmann, P. Zacke, D. Chatterjee, C. Correa, O. Deutschmann, L. Maier, S. Tischer, J. Warnatz, *SAE Technical Paper* **2002**, 2002-01-0065.
- [99] U. Tuttlies, V. Schmeisser, G. Eigenberger, *Chemical Engineering Science* **2004**, 59, 4731.
- [100] V. Schmeisser, G. Eigenberger, U. Nieken, *Topics in Catalysis* **2009**, 52, 1934.
- [101] X. Yan, U. Maas, *Proceedings of the Combustion Institute* **2000**, 28, 1615.
- [102] M. Votsmeier, *Chemical Engineering Science* **2009**, 64, 1384.
- [103] M. Votsmeier, A. Scheuer, A. Drochner, H. Vogel, J. Gieshoff, *Catalysis Today* **2009**, 151, 271.
- [104] J. Warnatz, *Proc. Combust. Inst.* **1981**, 18, 369.
- [105] R. W. D. J. Warnatz, U. Maas, Springer-Verlag, New York, **1996**.
- [106] C. T. B. J. A. Miller, *Prog. Ener. Combust. Sci.* **1989**, 15, 287.
- [107] W. H. Frenklach M, Yu C.L, Goldenberg M, Bowman C.T, Hanson R.K, et al., **1995**, <http://web.galcit.caltech.edu/EDL/mechanisms/library>; <http://diesel.me.berkeley.edu/wgri_mech/new21/>.
- [108] G. P. Smith, Golden, D.M., Frenklach, M., Moriarty, N.W., Eiteneer, B., Goldenberg, M., Bowman, C.T., Hanson, R.K., Song, S., Gardiner Jr., W.C., Lissianski, V.V., Qin, .W., <http://www.me.berkeley.edu/gri_mech/> **1999**.
- [109] V. V. L. Z. Qin, H. Yang, W. C. Gardiner, S. G. Davis, H. Wang, *Proc. Combust. Inst.* **2000**, 28, 1663.
- [110] A. Konnov, <http://homepages.vub.ac.be/~akonnov> **2000**.
- [111] S. K. Hidaka Y, Henmi Y, Tanaka H, Inami K. , *Combust. Flame* **1999**, 118, 340.
- [112] S. K. Hidaka Y, Hoshikawa H, Nihimori T, Takahashi R, Tanaka H, et al., *Combust. Flame* **2000**, 120, 245.
- [113] T. T. K. J. Hughes, A. Clague, M. J. Pilling, *Int. J. Chem. Kinet* **2001**, 33, 513.
- [114] B. Eiteneer, Frenklach, M., *International Journal of Chemical Kinetics* **2003**, 35, 391.
- [115] D. P. El Bakali A, Pillier L, Desgroux P, Pauwels J.F, Rida A, et al., *Combust. Flame* **2004**, 137, 109.
- [116] W. F. A. Petrova M.V, *Combust. Flame* **2006**, 144, 526.
- [117] B. W. K. Huang J, *Combust. Flame* **2006**, 144, 74.
- [118] E. Ranzi, et al., <http://www.chem.polimi.it/CRECKModeling/kinetic.html> **2007**.
- [119] D. Healy, Curran, H.J., Dooley, S., Simmie, J.M., Kalitan, D.M., Petersen, E.L., Bourque, G., *Combustion and Flame* **2008**, 155, 451.
- [120] D. Healy, Curran, H.J., Simmie, J.M., Kalitan, D.M., Zinner, C.M., Barrett, A.B., Petersen, E.L., Bourque, G., *Combust. Flame* **2008**, 155, 441.

- [121] H. E. Gupta GK, Zhu H, Dean AM, Kee RJ, *J Power Sources* **2006**, 156, 434.
- [122] J. W. M. Frenklach, *Combust. Sci. Tech* **1987**, 51, 265.
- [123] E. A. M. Maryam Younessi-Sinaki, Feridun Hamdullahpur *International Journal of Hydrogen Energy* **2009**, 34, 3710
- [124] B. H. Appel J, Frenklach M., *Combust. Flame* **2000**, 121, 122.
- [125] K. Norinaga, O. Deutschmann, *Ind. Eng. Chem. Res.* **2007**, 46, 3547.
- [126] P. G. H. J. Curran, W. J. Pitz, C. K. Westbrook, *Combust. Flame* **2002**, 129, 253.
- [127] V. C. P. A. Glaude, R. Fournet, F. Battin-Leclerc, G. M. Come, G. Scacchi, P. Dagaut, M. Cathonnet, *Energy & Fuels* **2002**, 16, 1186.
- [128] F. T. V. I. Golovitchev, L. Chomial, *SAE paper 1999-01-3552*; <http://www.tfd.chalmers.se/~valeri/MECH.html> **1999**.
- [129] F. Battin-Leclerc, R. Fournet, P. A. Glaude, B. Judenherc, V. Warth, G. M. Côme, G. Scacchi, *Proceedings of the Combustion Institute* **2000**, 28, 1597.
- [130] G. Bikas, N. Peters, *Combustion and Flame* **2001**, 126, 1456.
- [131] <http://www.enisc.u-nancy.fr/ENSIC/DCPR/global/accueil.html>.
- [132] V. P. Zhdanov, B. Kasemo, *Surface Science Reports* **1994**, 20, 111.
- [133] P. R. Norton, in *The Chemical Physics of Solid Surfaces and Heterogeneous Catalysis, Vol. 4* (Eds.: D. A. King, D. P. Woodroft), Elsevier, Amsterdam, **1982**.
- [134] J. L. Gland, G. B. Fisher, E. B. Kollin, *Journal of Catalysis* **1982**, 77, 263.
- [135] H. K. T. Engel, *Surface Science* **1979**, 90, 181.
- [136] K. M. Ogle, J. M. White, *Surface Science* **1984**, 139, 43.
- [137] J. Warnatz, M. D. Allendorf, R. J. Kee, M. E. Coltrin, *Combustion and Flame* **1994**, 96, 393.
- [138] Y. K. Park, P. Aghalayam, D. G. Vlachos, *Journal of Physical Chemistry A* **1999**, 103, 8101.
- [139] P. A. Bui, D. G. Vlachos, P. R. Westmoreland, *Surface Science* **1997**, 385, L1029.
- [140] A. R. R.A. van Santen, R.J. Gelten, *Stud. Surf. Sci. Catal.* **1997**, 109, 61.
- [141] D. K. M. Rinnemo, S. Johansson, K.L. Wong, V.P. Zhdanov, B. Kasemo, *Surface Science* **1997**, 276, 297.
- [142] M. P. Harold, M. E. Garske, *Journal of Catalysis* **1991**, 127, 553.
- [143] P. Aghalayam, Y. K. Park, D. G. Vlachos, in *Proc. Combust. Inst., Vol. 28*, Edinburgh, Scotland, **2000**.
- [144] M. P. Harold, M. E. Garske, *Journal of Catalysis* **1991**, 127, 524.
- [145] M. P. H. M.E. Garske, *Chem. Eng. Sci.* **1992**, 47, 623.
- [146] D. A. Hickman, L. D. Schmidt, *AIChE Journal* **1993**, 39, 1164.
- [147] O. Deutschmann, F. Behrendt, J. Warnatz, *Catalysis Today* **1994**, 21, 461.
- [148] M. P. Z. Mallen, W.R. Williams, L.D. Schmidt, *J. Phys. Chem.* **1993**, 97, 625.
- [149] O. Deutschmann, L. Maier, U. Riedel, A. H. Stroemann, R. W. Dibble, *Catalysis Today* **2000**, 59, 141.
- [150] D. A. Hickman, E. A. Haupfear, L. D. Schmidt, *Catalysis Letters* **1993**, 17, 223.
- [151] R. Quiceno, J. Perez-Ramirez, J. Warnatz, O. Deutschmann, *Applied Catalysis a-General* **2006**, 303, 166.
- [152] R. D. Cortright, S. A. Goddard, J. E. Rekoske, J. A. Dumesic, *Journal of Catalysis* **1991**, 127, 342.
- [153] S. A. Goddard, R. D. Cortright, J. A. Dumesic, *Journal of Catalysis* **1992**, 137, 186.
- [154] M. C. Huff, L. D. Schmidt, *Aiche Journal* **1996**, 42, 3484.
- [155] R. S. Vincent, R. P. Lindstedt, N. A. Malik, I. A. B. Reid, B. E. Messenger, *Journal of Catalysis* **2008**, 260, 37.
- [156] J. A. Dumesic, A. A. Trevino, *Journal of Catalysis* **1989**, 116, 119.
- [157] P. Stoltze, J. K. Nørskov, *Physical Review Letters* **1985**, 55.
- [158] I. P. M. Bowker, K.C. Waugh, *Applied Catalysis* **1985**, 14, 101.

- [159] M. Bowker, I. Parker, K. C. Waugh, *Surface Science* **1988**, *197*, L223.
- [160] T. Pignet, L. D. Schmidt, *Chemical Engineering Science* **1974**, *29*, 1123.
- [161] J. Koop, O. Deutschmann, *Applied Catalysis B-Environmental* **2009**, *91*, 47.
- [162] L. D. S. S.B. Schwartz, G.B. Fisher, , *J. Phys. Chem.* **1986**, *90*, 6194.
- [163] S. H. Oh, G. B. Fisher, J. E. Carpenter, D. W. Goodman, *Journal of Catalysis* **1986**, *100*, 360.
- [164] S. H. O. G.B. Fisher, J.E. Carpenter, C.L. DiMaggio, S.J. Schmiege, in: A. Crucq, A. Frenet *Catalysis and Automotive Pollution Control*, **1987**.
- [165] O. Deutschmann, R. Schwiedernoch, L. I. Maier, D. Chatterjee, *Studies in Surface Science and Catalysis* **2001**, *136*, 251.
- [166] M. Maestri, D. G. Vlachos, A. Beretta, P. Forzatti, G. Groppi, E. Tronconi, *Topics in Catalysis* **2009**, *52*, 1983.
- [167] A. B. Mhadeshwar, D. G. Vlachos, *The Journal of Physical Chemistry B* **2005**, *109*, 16819.
- [168] M. Maestri, D. G. Vlachos, A. Beretta, G. Groppi, E. Tronconi, *Journal of Catalysis* **2008**, *259*, 211.
- [169] J. Thormann, L. Maier, P. Pfeifer, U. Kunz, O. Deutschmann, K. Schubert, *International Journal of Hydrogen Energy* **2009**, *34*, 5108.
- [170] B. T. Schadel, M. Duisberg, O. Deutschmann, *Catalysis Today* **2009**, *142*, 42.
- [171] V. P. Zhdanov, B. Kasemo, *Catalysis Letters* **1996**, *40*, 197.
- [172] D. N. Belton, S. J. Schmiege, *Journal of Catalysis* **1992**, *138*, 70.
- [173] M. Hartmann, L. Maier, H. D. Minh, O. Deutschmann, *Combustion and Flame* **2010**, *157*, 1771.
- [174] K. Y. S. Ng, D. N. Belton, S. J. Schmiege, G. B. Fisher, *Journal of Catalysis* **1994**, *146*, 394.
- [175] J. Xu, M. P. Harold, V. Balakotaiah, *Applied Catalysis B: Environmental* **2009**, *89*, 73.
- [176] J. F. Kramer, S. A. S. Reihani, G. S. Jackson, *Proceedings of the Combustion Institute* **2003**, *29*, 989.
- [177] S. A. Seyed-Reihani, G. S. Jackson, *Chemical Engineering Science* **2004**, *59*, 5937.
- [178] C. Stegelmann, N. C. Schjødt, C. T. Campbell, P. Stoltze, *Journal of Catalysis* **2004**, *221*, 630.
- [179] C. V. Ovesen, B. S. Clausen, B. S. Hammershøi, G. Steffensen, T. Askgaard, I. Chorkendorff, J. K. Nørskov, P. B. Rasmussen, P. Stoltze, P. Taylor, *Journal of Catalysis* **1996**, *158*, 170.
- [180] K. C. Waugh, *Chem. Eng. Sci.* **1996**, *51*, 1533.
- [181] K. C. W. E. Tserpe, *Stud. Surf. Sci. Catal.* **1997**, *109*, 401.
- [182] C. V. Ovesen, P. Stoltze, J. K. Nørskov, C. T. Campbell, *Journal of Catalysis* **1992**, *134*, 445.
- [183] K.-H. Ernst, C. T. Campbell, G. Moretti, *Journal of Catalysis* **1992**, *134*, 66.
- [184] P. B. Rasmussen, P. M. Holmblad, T. Askgaard, C. V. Ovesen, P. Stoltze, J. K. Nørskov, I. Chorkendorff, *Catalysis Letters* **1994**, *26*, 373.
- [185] T. S. Askgaard, J. K. Nørskov, C. V. Ovesen, P. Stoltze, *Journal of Catalysis* **1995**, *156*, 229.
- [186] L. M. Aparicio, *Journal of Catalysis* **1997**, *165*, 262.
- [187] D. W. Blaylock, T. Ogura, W. H. Green, G. J. O. Beran, *The Journal of Physical Chemistry C* **2009**, *113*, 4898.

TABLE CAPTIONS

Table 1: Approaches for modeling rates of heterogeneous catalytic reactions.

Table 2: Selection of homogeneous reaction mechanisms relevant for modeling catalytic reactors.

Table 3: Thermodynamically consistent surface reaction mechanism for steam-reforming of methane over nickel-based catalysts^[57]; parameter definition according to Eq. (4.4).

Table 4: Selection of heterogeneous reaction mechanisms using the mean-field approach.

Table 1:

Method of modeling	Simplification	Application
Ab-initio calculation	Most fundamental approach	Simple chemical systems
Density functional theory (DFT)	Replacement of the N-electron wave function by the electron density	Dynamics of reactions, activation barriers, adsorbed structures, frequencies
(Kinetic) Monte Carlo	Details of dynamics neglected	Adsorbate - adsorbate interactions on catalytic surfaces and nanoparticles
Mean-field approximation (MF)	Details on adsorbate structure neglected	Microkinetic modeling of catalytic reactions in technical systems
Langmuir-Hinshelwood-Hougen-Watson (LHHW)	Rate-determining step needed	Modeling of catalytic reactions in technical systems
Power-law kinetics	All mechanistic aspects neglected	Scale-up and reactor design for "black-box" systems

Table 2:

	Number species/ir-reversible reactions	Mechanism type / species considered	Range of conditions
Warnatz 1981 ^[104, 105]	26/189	C1-C2	methane and natural gas combustion
Miller/Bowman 1989 ^[106]	.../141	C1-C4	methane and natural gas combustion
GRI 1.2 (Frenklach) 1995 ^[107]	25/168	C1-C2	natural gas flames and ignition, flame propagation
GRI 3.0 (Smith/Golden/Frenklach) 1999 ^[108]	53/325	C1-C3	1000–2500 K, 1.0–1000 kPa, equivalence ratios: $\Phi = 0.1-5$ for premixed systems
Qin 2000 ^[109]	.../258	C1-C3	propane flame speed and ignition
Konnov 2000 ^[110]	127/1200	C1-C3, OH, NO _x , and NH ₃ kinetics	species profiles in flow reactor, ignition delay times in shock waves, laminar flame speed and species profiles
Hidaka/Tanaka 2000 ^[111, 112]	48/157	C1-C2	reflected shock waves 1350–2400 K, 162–446 kPa.
Leeds 1.4 (Hughes) 2001 ^[113]	37/351	C1-C2	species profiles in laminar flames, flame speeds, ignition delay
GRI extended (Eiteneer/Frenklach) 2003 ^[114]	71/486	C1-C3 (GRI 3.0) + C ₂ H _x , C ₃ H _x , C ₄ H _x	acetylene ignition in shock tubes
GDF-Kin (El Bakali/Dagaut) 2004 ^[115]	99/671	C1-C6	laminar flame speeds, jet stirred reactor at 1 atm, $\Phi = 0.75 : 1.0 : 1.5$
San Diego 2006 ^[116]	86/362	C1-C3 (excluding low-temperature fuel-peroxide kinetics)	below about 100 atm, above about 1000 K, $\Phi < 3$, deflagration velocities and shock-tube ignition.
UBC 2.0 2006 ^[117]	55/278	C1-C2 (GRI 1.2) + C ₃ + CH ₃ O ₂ , C ₂ H ₅ O ₂ , C ₃ H ₇ O ₂	ignition delay in reflected-shock, 900-1400 K, 16- 40 bar.
Ranzi 2007 ^[118]	79/1377	C1-C3	high temperature pyrolysis, partial oxidation and combustion
Healy/Curran 2008 ^[119, 120]	289/3128	C1-C3	740–1550 K, 10 - 30 atm, $\Phi = 0.3 - 3.0$ in a high-pressure shock tube and in a rapid compression machine.
Gupta 2006 ^[121]	190/1150	C1-C6 + Frenklach/Warnatz 1987 soot model ^[122]	low temperature pyrolysis in fuel cells (900–1200K)
Younessi-Sinaki 2009 ^[123]	75/242	C1-C2 (GRI 1.2) + C>2 (excluding the oxygenates) + Appel 2000 soot model ^[124]	homogeneous thermal (oxygen free) decomposition
Norinaga 2007 ^[125]	227/827	C1-C4 + Frenklach/Warnatz 1987 soot model ^[122]	Pyrolysis, flow reactor at 900 °C, pressures of 2-15 kPa, and residence times of up to 1.6 s.
LLNL 2002 ^[126]	857/3606	C1-C8	550-1700K; 1-45 bar; 70-99% N ₂ (Ar)
Glaude 2002 ^[127]	367/1832	C1-C8	500-1100K; 1-20 bar
Golovitchev 1999 ^[128]	130/690	C1-C8	640-1760K; 1-55 bar; 76-95% Ar
Battin-Leclerc 2000 ^[129]	.../7920	C1-C10	jet-stirred reactor, premixed laminar flame, 550K – 1600K
Bikas/Peters 2001 ^[130]	67/600	C1-C10	premixed flame at 100 kPa, flat flames, shock waves, jet-stirred reactor
Ristori/Dagaut 2001 ^[28]	242/1801	C1-C16	jet-stirred reactor, 1000K - 1250 K, 100 kPa, residence time of 70 ms, $\Phi = 0.5, 1, \text{ and } 1.5$.
Nancy 2001 ^[131]	265/1787	C1-C16	jet-stirred reactor, 1000K - 1250 K

Table 3:

	REACTION	A/[cm, mol, s]	E _a /[kJ/mol]	β [-]
R1	H ₂ + 2 Ni(s) → 2 H(s)	1.000·10 ⁻⁰²	0.0	0.0
R2	2 H(s) → 2 Ni(s) + H ₂	2.545·10 ⁺¹⁹	81.21	0.0
R3	O ₂ + 2 Ni(s) → 2 O(s)	1.000·10 ⁻⁰²	0.0	0.0
R4	2 O(s) → 2 Ni(s) + O ₂	4.283·10 ⁺²³	474.95	0.0
R5	CH ₄ + Ni(s) → CH ₄ (s)	8.000·10 ⁻⁰³	0.0	0.0
R6	CH ₄ (s) → CH ₄ + Ni(s)	8.705·10 ⁺¹⁵	37.55	0.0
R7	H ₂ O + Ni(s) → H ₂ O(s)	1.000·10 ⁻⁰¹	0.0	0.0
R8	H ₂ O(s) → H ₂ O + Ni(s)	3.732·10 ⁺¹²	60.79	0.0
R9	CO ₂ + Ni(s) → CO ₂ (s)	1.000·10 ⁻⁰⁵	0.0	0.0
R10	CO ₂ (s) → CO ₂ + Ni(s)	6.447·10 ⁺⁰⁷	25.98	0.0
R11	CO + Ni(s) → CO(s)	5.000·10 ⁻⁰¹	0.0	0.0
R12	CO(s) → CO + Ni(s)	3.563·10 ⁺¹¹	111.27-50θ _{CO(s)}	0.0
R13	CH ₄ (s) + Ni(s) → CH ₃ (s) + H(s)	3.700·10 ⁺²¹	57.7	0.0
R14	CH ₃ (s) + H(s) → CH ₄ (s) + Ni(s)	6.034·10 ⁺²¹	61.58	0.0
R15	CH ₃ (s) + Ni(s) → CH ₂ (s) + H(s)	3.700·10 ⁺²⁴	100.0	0.0
R16	CH ₂ (s) + H(s) → CH ₃ (s) + Ni(s)	1.293·10 ⁺²³	55.33	0.0
R17	CH ₂ (s) + Ni(s) → CH(s) + H(s)	3.700·10 ⁺²⁴	97.10	0.0
R18	CH(s) + H(s) → CH ₂ (s) + Ni(s)	4.089·10 ⁺²⁴	79.18	0.0
R19	CH(s) + Ni(s) → C(s) + H(s)	3.700·10 ⁺²¹	18.8	0.0
R20	C(s) + H(s) → CH(s) + Ni(s)	4.562·10 ⁺²²	161.11	0.0
R21	CH ₄ (s) + O(s) → CH ₃ (s) + OH(s)	1.700·10 ⁺²⁴	88.3	0.0
R22	CH ₃ (s) + OH(s) → CH ₄ (s) + O(s)	9.876·10 ⁺²²	30.37	0.0
R23	CH ₃ (s) + O(s) → CH ₂ (s) + OH(s)	3.700·10 ⁺²⁴	130.1	0.0
R24	CH ₂ (s) + OH(s) → CH ₃ (s) + O(s)	4.607·10 ⁺²¹	23.62	0.0
R25	CH ₂ (s) + O(s) → CH(s) + OH(s)	3.700·10 ⁺²⁴	126.8	0.0
R26	CH(s) + OH(s) → CH ₂ (s) + O(s)	1.457·10 ⁺²³	47.07	0.0
R27	CH(s) + O(s) → C(s) + OH(s)	3.700·10 ⁺²¹	48.1	0.0
R28	C(s) + OH(s) → CH(s) + O(s)	1.625·10 ⁺²¹	128.61	0.0
R29	H(s) + O(s) → OH(s) + Ni(s)	5.000·10 ⁺²²	97.9	0.0
R30	OH(s) + Ni(s) → H(s) + O(s)	1.781·10 ⁺²¹	36.09	0.0
R31	H(s) + OH(s) → H ₂ O(s) + Ni(s)	3.000·10 ⁺²⁰	42.7	0.0
R32	H ₂ O(s) + Ni(s) → H(s) + OH(s)	2.271·10 ⁺²¹	91.76	0.0
R33	OH(s) + OH(s) → H ₂ O(s) + O(s)	3.000·10 ⁺²¹	100.0	0.0
R34	H ₂ O(s) + O(s) → OH(s) + OH(s)	6.373·10 ⁺²³	210.86	0.0
R35	C(s) + O(s) → CO(s) + Ni(s)	5.200·10 ⁺²³	148.1	0.0
R36	CO(s) + Ni(s) → C(s) + O(s)	1.354·10 ⁺²²	116.12-50θ _{CO(s)}	-3.0
R37	CO(s) + O(s) → CO ₂ (s) + Ni(s)	2.000·10 ⁺¹⁹	123.6-50θ _{CO(s)}	0.0
R38	CO ₂ (s) + Ni(s) → CO(s) + O(s)	4.653·10 ⁺²³	89.32	-1.0
R39	CO(s) + H(s) → HCO(s) + Ni(s)	4.019·10 ⁺²⁰	132.23	-1.0
R40	HCO(s) + Ni(s) → CO(s) + H(s)	3.700·10 ⁺²¹	0.0+50θ _{CO(s)}	0.0
R41	HCO(s) + Ni(s) → CH(s) + O(s)	3.700·10 ⁺²⁴	95.8	-3.0
R42	CH(s) + O(s) → HCO(s) + Ni(s)	4.604·10 ⁺²⁰	109.97	0.0

Table 4

Catalyst	Reactants & Products	Systems/Reactor configurations primarily ^{a)}
Pt	H ₂ /O ₂ &H ₂ O	Pt(111) ^[132-136] , Pt foil ^[71, 72, 137] , wire ^[73] , plate ^{[68][70]} , Pt ^[138, 139]
Pt	CO/O ₂ &CO ₂	Pt(100) ^[140] , Pt(111) ^[141] , Pt(110) ^[142] , Pt ^{[73][143]} , Pt wire ^[144, 145]
Pt	CH ₄ /O ₂ &H ₂ , CO, CO ₂ , H ₂ O	Pt foil ^[53, 146, 147] , Pt ^[71, 83, 148] , Pt/Al ₂ O ₃ monolith ^{[146, 149] [150]} , Pt gauze ^[151]
Pt	C ₂ H ₄ /H ₂ &C ₂ H ₆	Single crystals ^{[2] [152] [153]}
Pt	C ₂ H ₆ /O ₂ &C ₂ H ₄	Pt coated monolith ^[7, 86, 154, 155]
Pt	N ₂ /H ₂ &NH ₃	Single crystal studies ^{[2, 156] [157] [158, 159]}
Pt	NH ₃ /O ₂ &NO, H ₂ O	Pt wire ^[160]
Pt	C ₃ H ₆ /CH ₄ /CO/NO _x &N ₂ , CO ₂ , H ₂ O	Three-way automotive catalyst, NO _x storage/reduction automotive catalyst ^[161]
Rh	H ₂ /O ₂ &H ₂ O	Rh foil ^[148]
Rh	CO/O ₂ &CO ₂	Rh(111) ^[162] , Rh/Al ₂ O ₃ ^[163, 164]
Rh	CH ₄ /O ₂ &H ₂ , CO, H ₂ O, CO ₂	Rh/Al ₂ O ₃ coated monoliths ^{[146] [150, 165] [87, 166]}
Rh	CH ₄ /H ₂ O/CO ₂ /&CO, H ₂	Flow reactor ^{[167] [168]}
Rh	CH ₄ /H ₂ O&CO, H ₂	Rh/Al ₂ O ₃ coated microreactor ^[169, 170] , channel ^[170]
Rh	CO/NO&CO ₂ , N ₂	Rh(111) ^[171] , Rh/Al ₂ O ₃ in automotive converters ^[163]
Rh	CO/N ₂ O&CO ₂ , N ₂	Rh(111) ^[172]
Rh	C ₃ H ₈ /O ₂ /H ₂ O&CO, H ₂	Rh/Al ₂ O ₃ monolith ^[173]
Pt/Rh	CO/NO&CO ₂ , N ₂	Flow reactor ^[174]
Pt/Rh/Al ₂ O ₃	C ₃ H ₆ /CO/NO&N ₂ , CO ₂ , H ₂ O	Three-way automotive catalyst ^[88]
Pt/BaO/Al ₂ O ₃	NO/NH ₃ /H ₂ &N ₂	NO _x storage and reduction automotive monolith catalysts ^[175]
Pd	H ₂ /O ₂ &H ₂ O	Pd wire ^[53] , coated microreactor ^[176, 177]
Ag	C ₂ H ₄ /O ₂ &C ₂ H ₄ O	kinetics of epoxidation, ethylene combustion, TPD, TPR ^[178]
Cu	CO/H ₂ O&H ₂ , CO ₂	Cu(111) ^{[179] [180, 181] [182]} , Cu(110) ^[183] , Cu/Al ₂ O ₃ ; SiO ₂ ^[179]
Cu	CO/H ₂ &CH ₃ OH	Cu(100) ^[184, 185]
Ni	CH ₄ /H ₂ O/CO ₂ &H ₂ , CO	Ni/MgAl ₂ O ₃ -MgO ^[186] , Ni/YSC ^[58] , Ni/Al ₂ O ₃ ^[57]
Ni	CH ₄ /H ₂ O&H ₂ , CO	Ni(111) ^[187]

a) Catalysts without crystal face denote polycrystalline material.

FIGURES CAPTIONS

Figure 1: Surface description by reactant and product patterns. a) Examples for the main processes occurring in catalysis. b) Incorporation of a hard sphere interaction specific with oxygen. c) Modelling of pair wise soft interactions with interaction energy tables. Adapted from ^[32, 33].

Figure 2: a) An extract from a surface model for a particle with a (100) and a (111) facet, linked along their common edge. b) A diffusion process for the (111) facet. c) A diffusion process across the facets. One matching position is marked green. Adapted from ^[32, 33].

Figure 3: Example for the matching of reactant pattern consisting of two parts M1 and M2: The surface consists of the two parts S1 and S2. The global application point for the reactant pattern is given by the position of M1 on S1 (red). From there, the local application point for M2 on S2 (green) can be derived as it is indicated by the arrows. Adapted from ^[32, 33].

Figure 4: a) Two supported nanoparticles surface model and b) view of the atoms for the c) lattice of the single particle model. Adapted from ^[32, 33].

Figure 5: Transition behavior of CO-oxidation on the single particle Pd-model. In the first 20s the particle was saturated with partial oxygen pressure of $p_{O_2} = 2 \cdot 10^{-7}$ mbar. After that additionally a CO partial pressure of $p_{CO} = 8 \cdot 10^{-7}$ mbar was applied. Top: reaction rate per unit cell per second (red) and its time average (black). Bottom: oxygen (blue) and CO (green) coverage. Adapted from ^[32, 33].

Figure 6: Reverse MC analysis: Each species is traced backwards from the particle, where it reactively desorbed to its original place, where it adsorbed. For periodic models the periodic boundary conditions have to be unfolded for species traveling across the boundary. This can be achieved by a two dimensional descriptor which is incremented or decremented during boundary passage. Taken from ^[33].

Figure 7: Capture zone of the black particle shown in the center. The number of adsorbed species, which later reactively desorb from the central particle, is counted for each individual adsorption site. Taken from ^[33].

Figure 8: Sketch of the major reaction steps in catalytic partial oxidation of methane over Rh applying the mean-field approximation^[87].

Figure 9: Illustration of the adjustment algorithm to set up thermodynamically consistent surface reaction mechanisms^[57].

Figure 10: Survey of the methodology of the development of a surface reaction mechanism^[55].

Figure 11: Sensitivity of the uncovered surface area on rate coefficients of surface reactions immediately before catalytic ignition of CH₄ oxidation on a platinum foil^[53].

Figure 12: Calculated time-dependent surface coverage and surface temperature during heterogeneous ignition of a CH₄/O₂/N₂ mixtures flowing in a stagnation-point flow onto a platinum foil^[53].

Figure 1

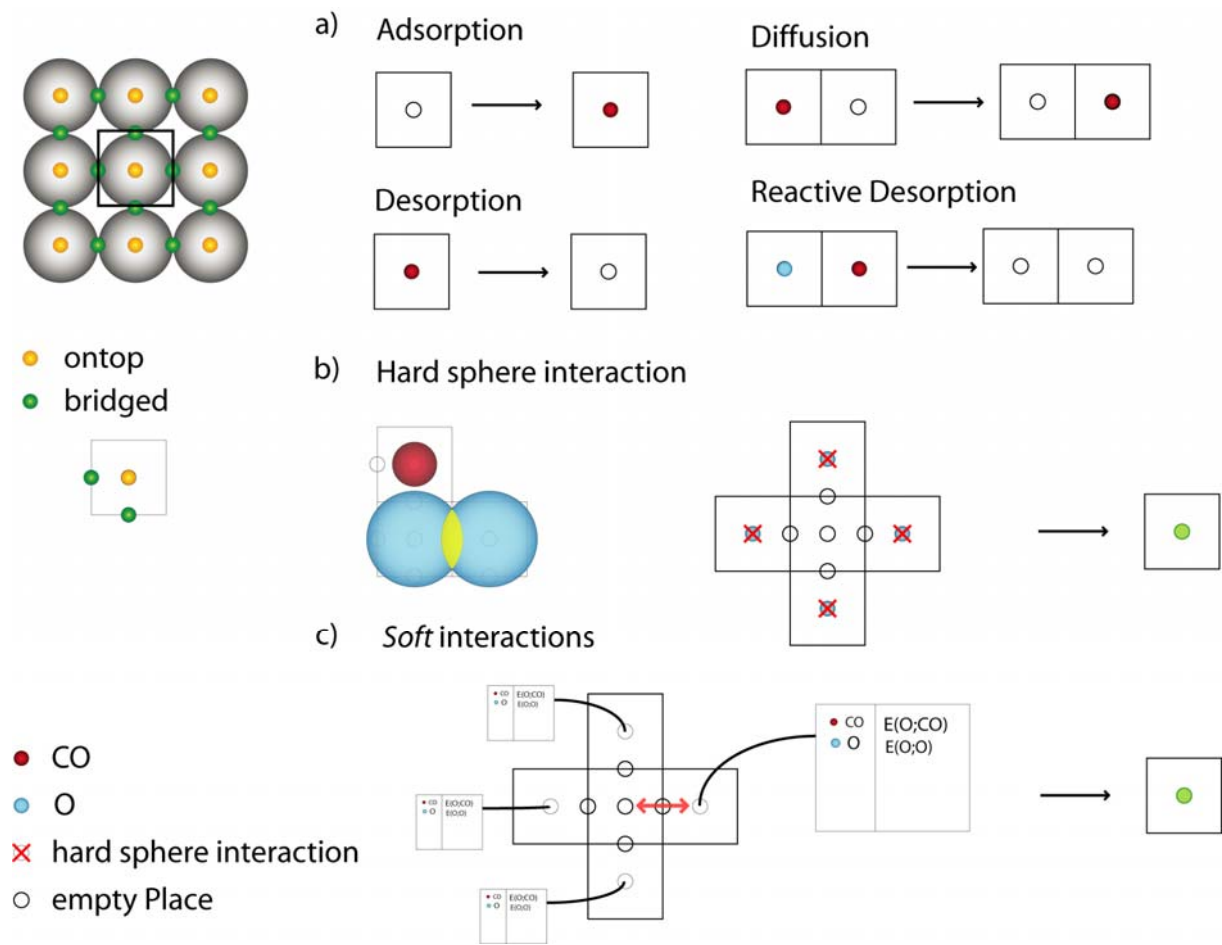


Figure 2:

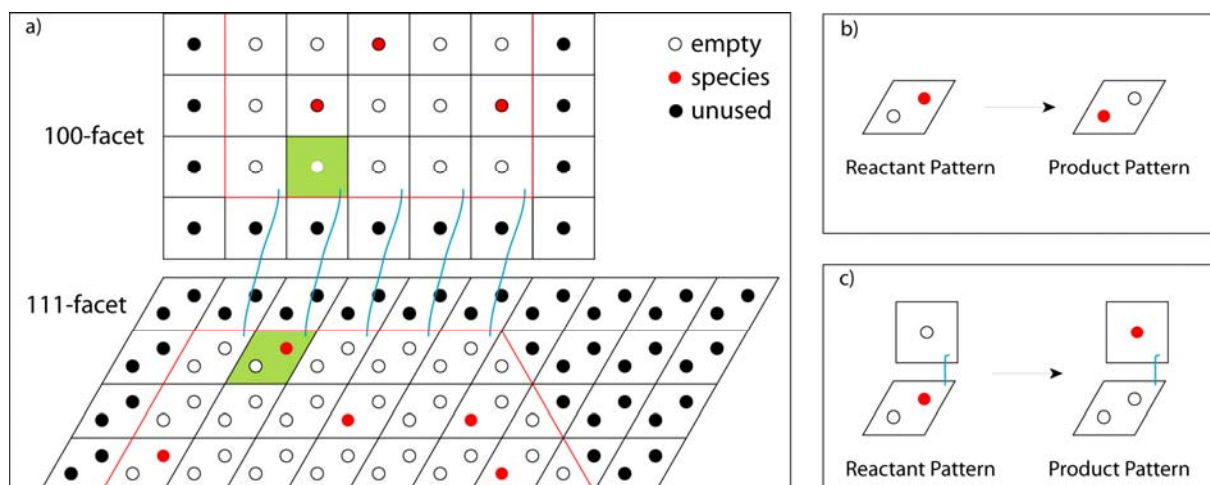


Figure 3:

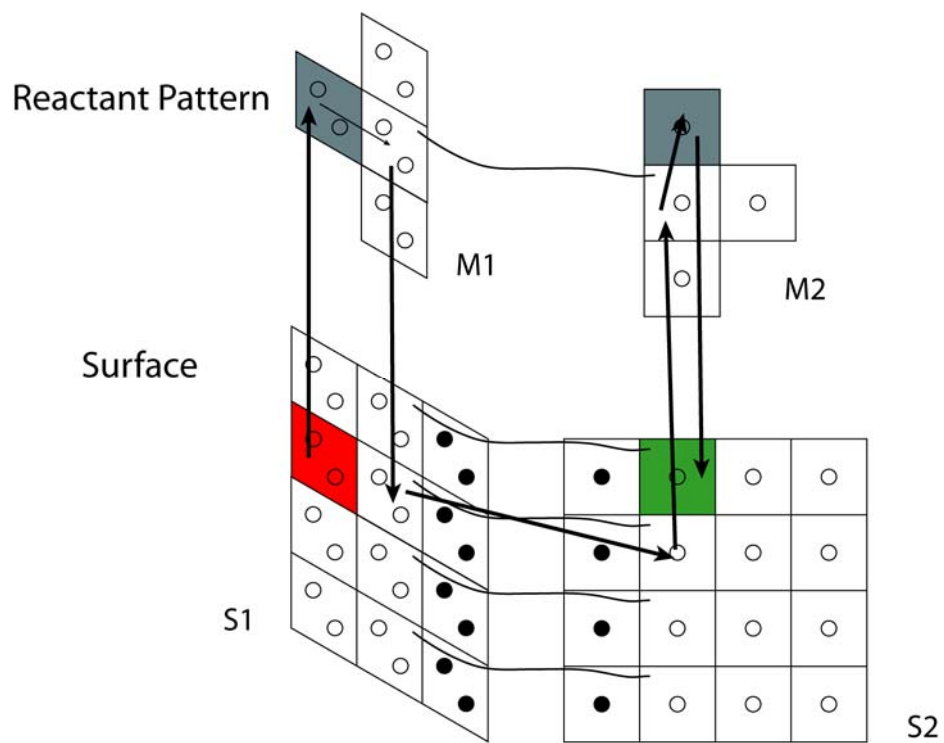


Figure 4:

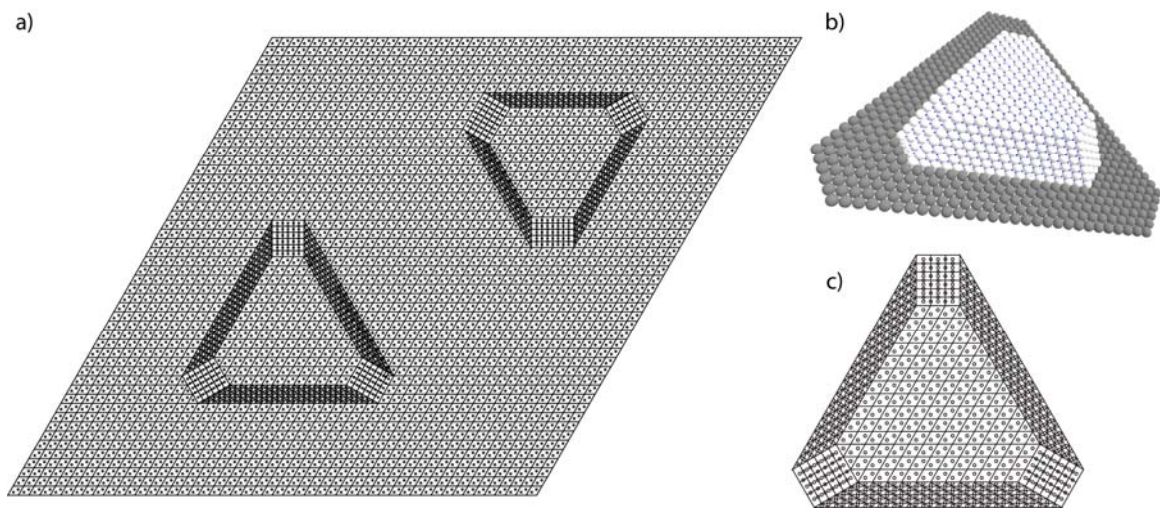


Figure 5:

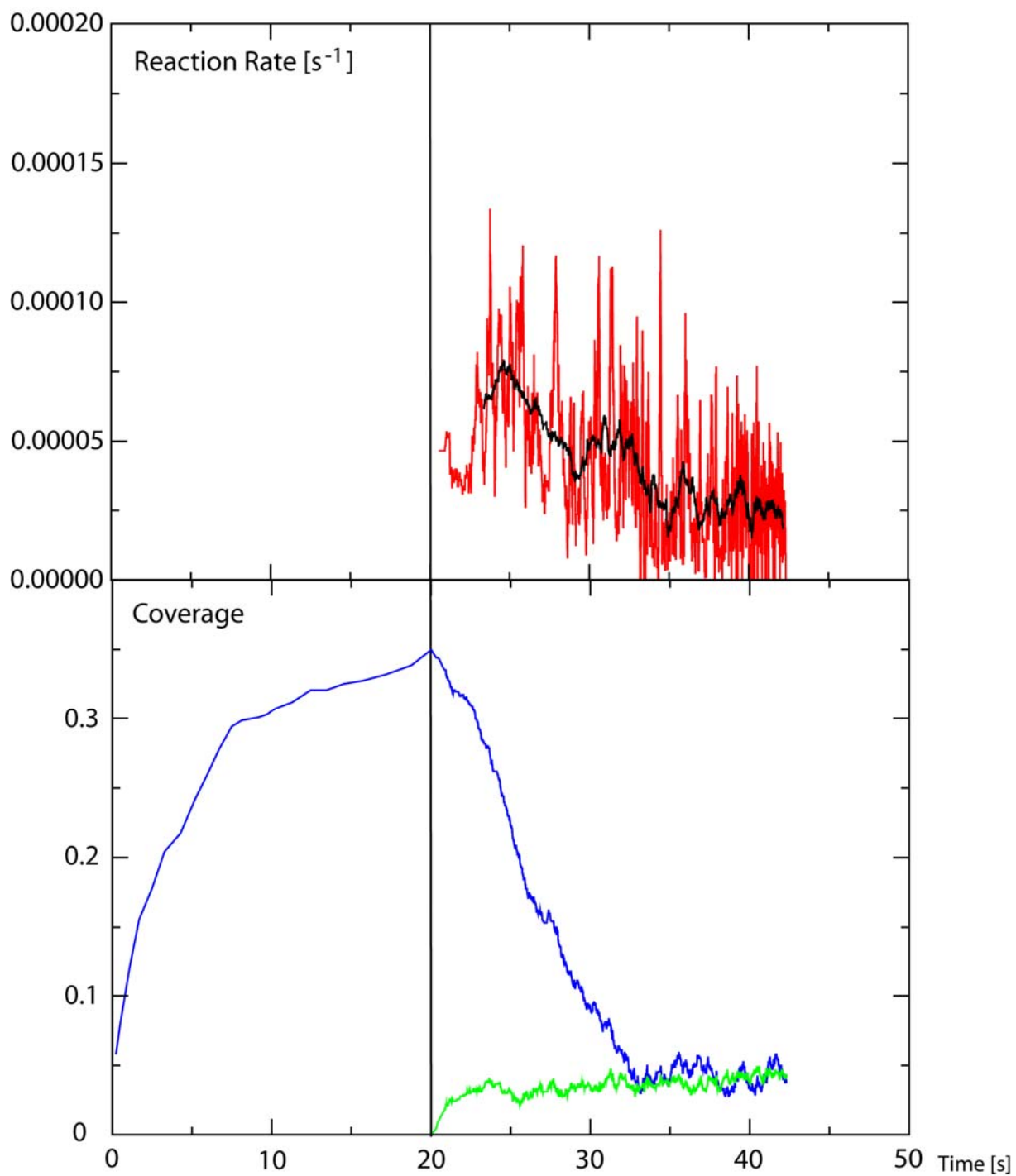


Figure 6:

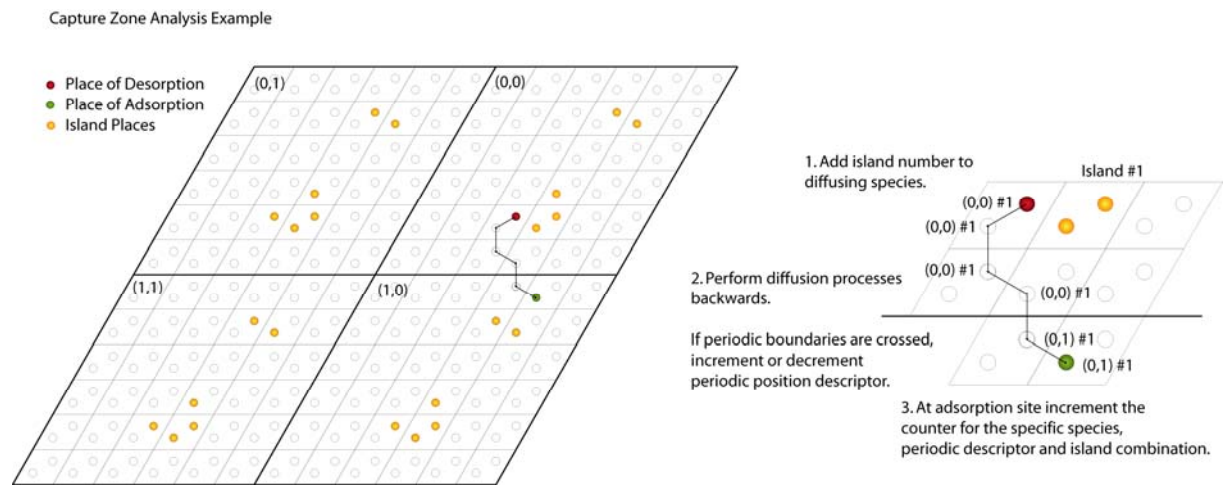


Figure 7:

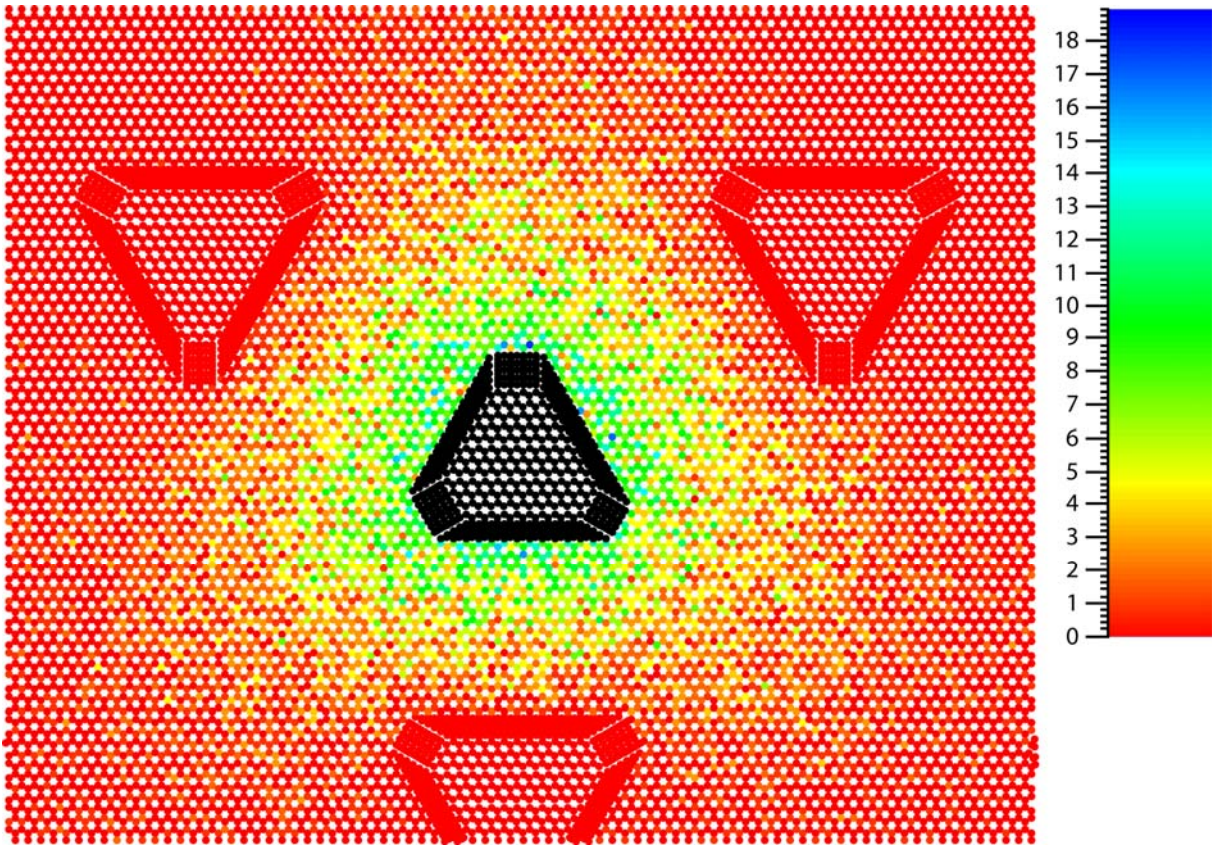


Figure 8:

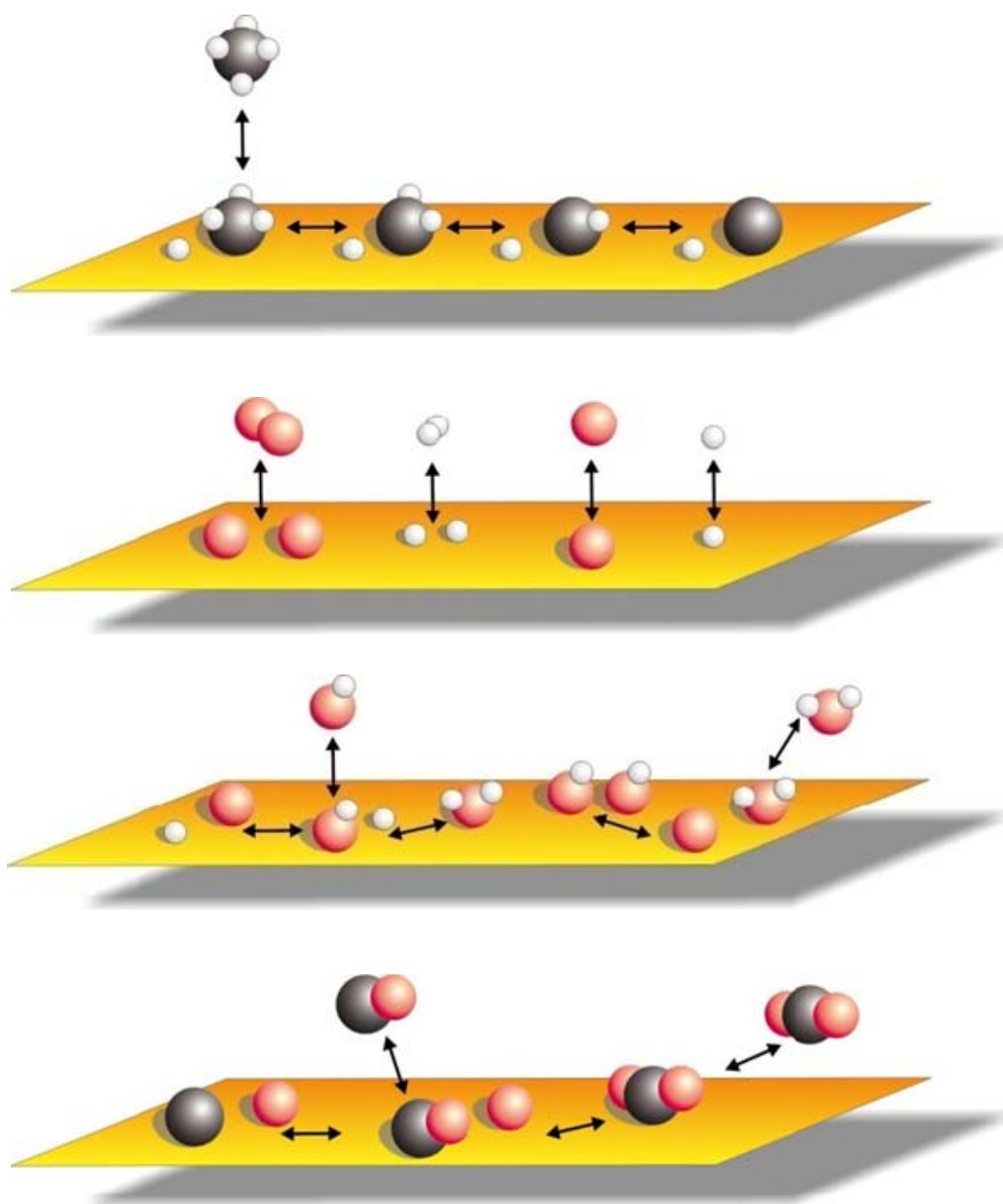


Figure 9:

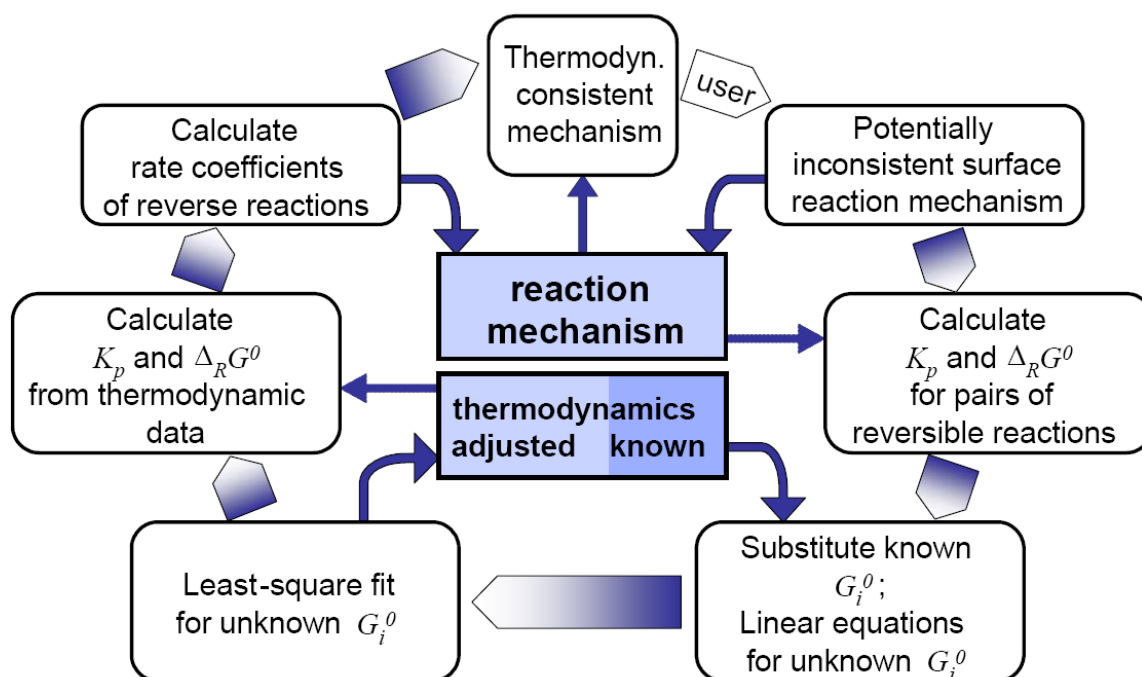


Figure 10:

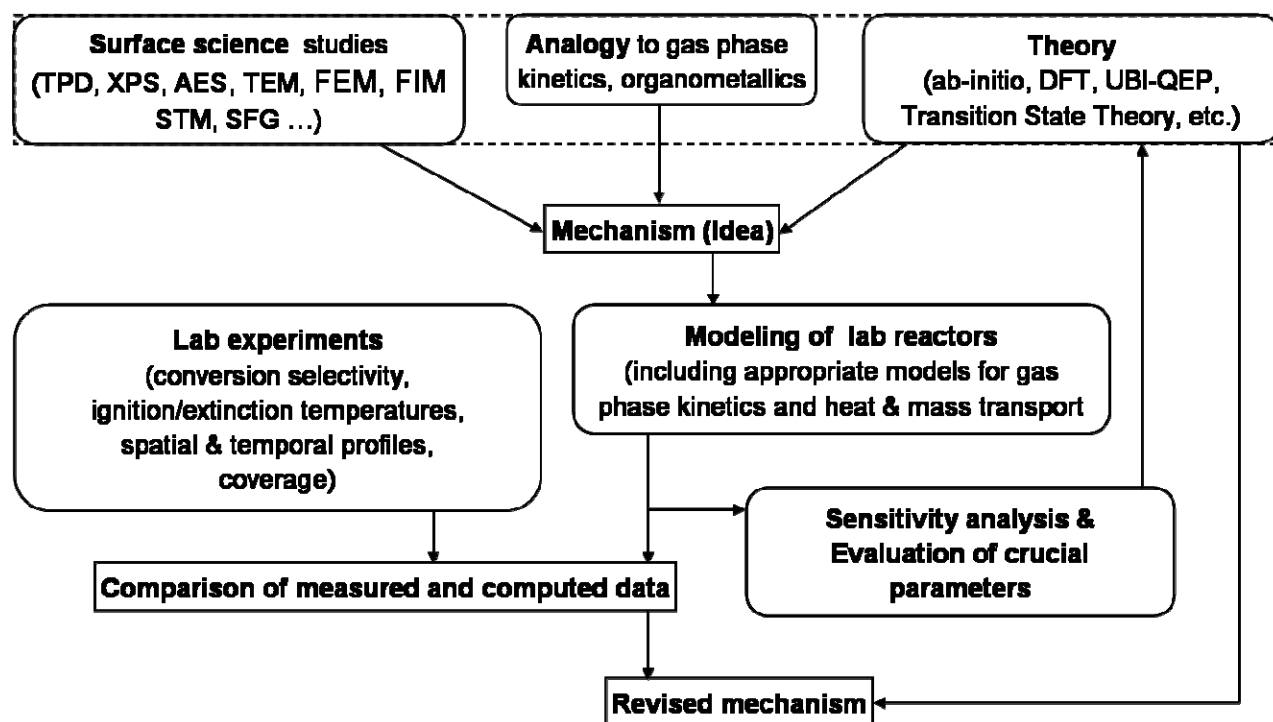


Figure 11:

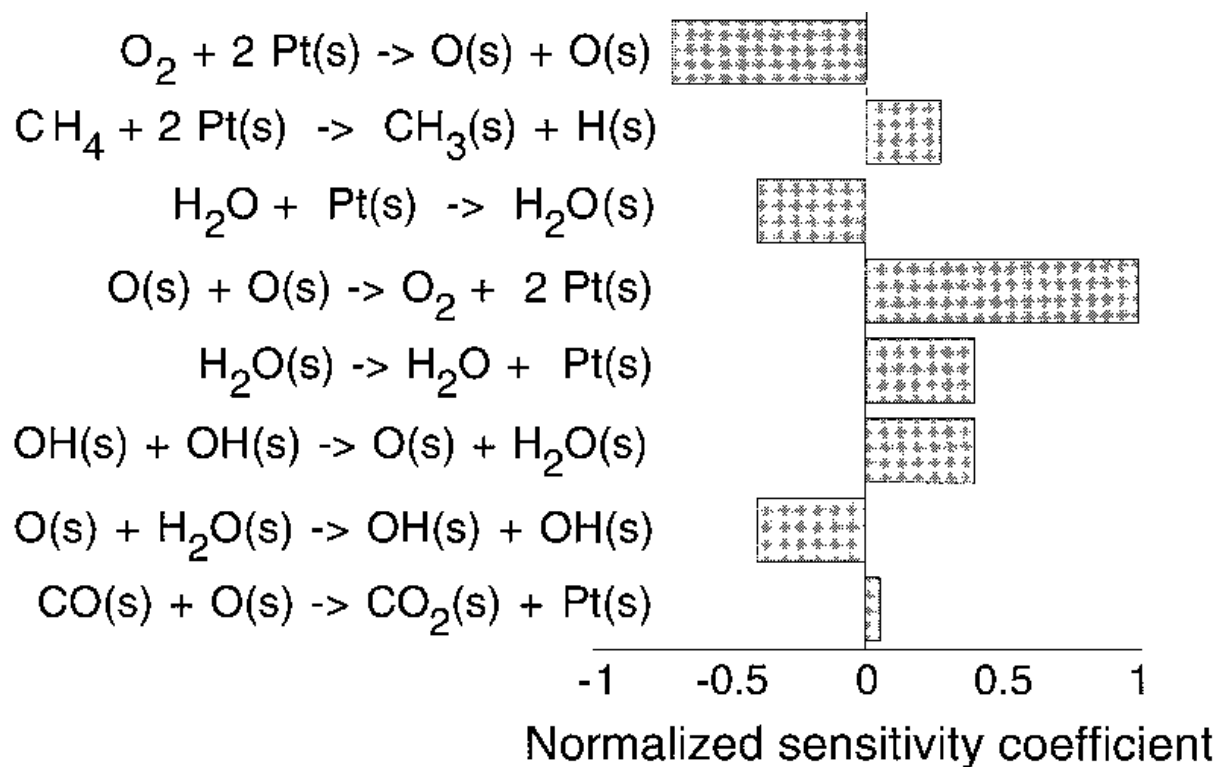


Figure 12:

